Séminaire Aristote "Quelles architectures pour les simulations de demain?
« 5 février 2015 Ecole Polytechnique (Palaiseau)

Aeromines: a new cloud computing platform

Elie Hachem*, Romain Klein, Alexandre Boilley, Youssef Mesri

CFL Computing and Fluids Research Team
MINES ParisTech – CEMEF
Sophia Antipolis, 60904 – France
elie.hachem@mines-paristech.fr

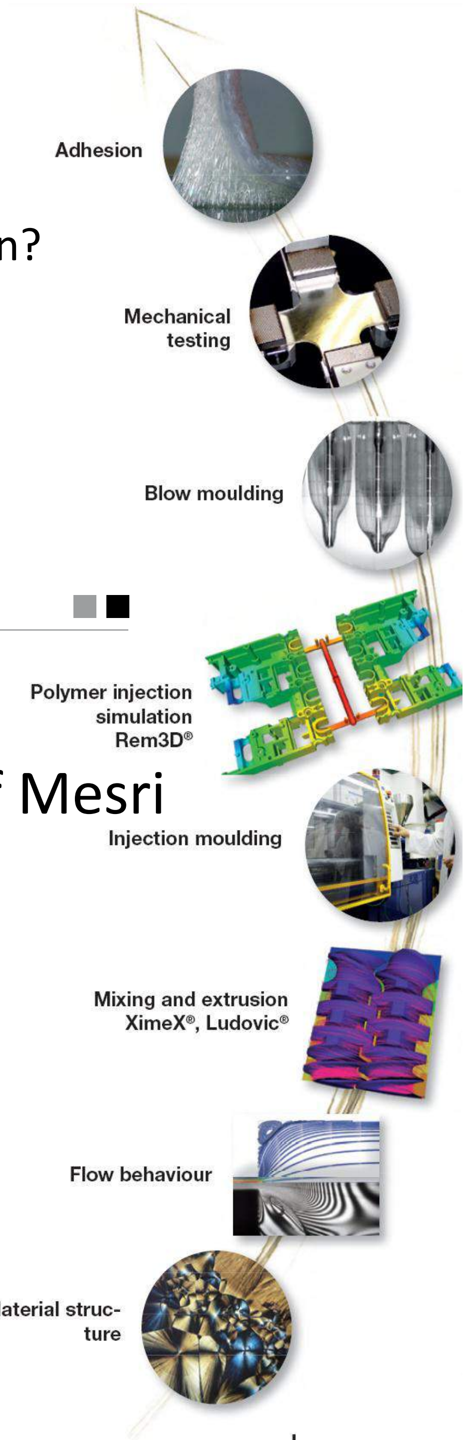

MINES ParisTech

Cemef

Challenges

- Industry is increasingly depending on advanced methods to fulfil the need to innovate in products and services

- Transition RANS→LES→DNS creates new opportunities for both science applications and computing technologies

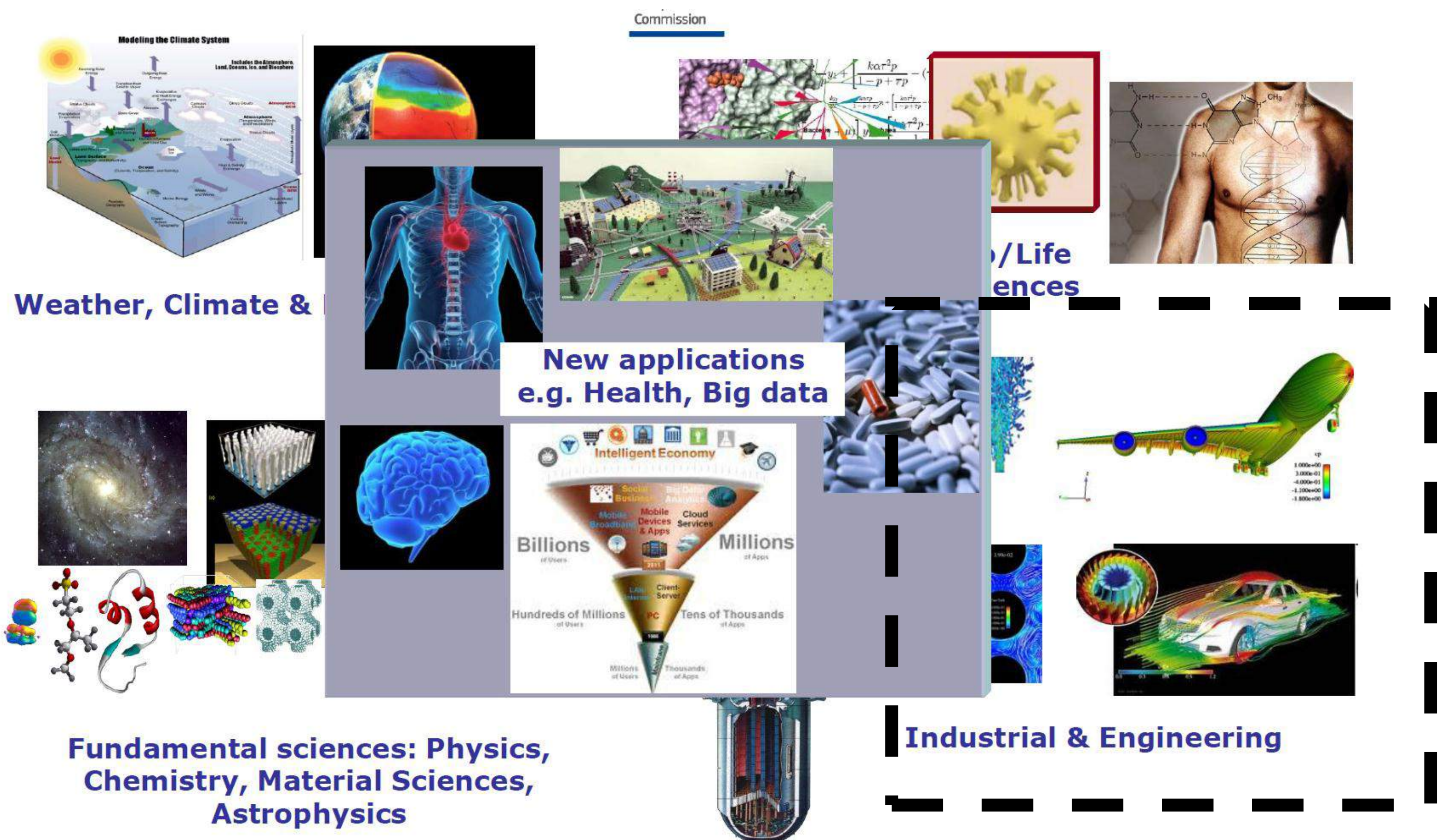

Taken from H2020 strategy report

Context

~2000 cores at CEMEF

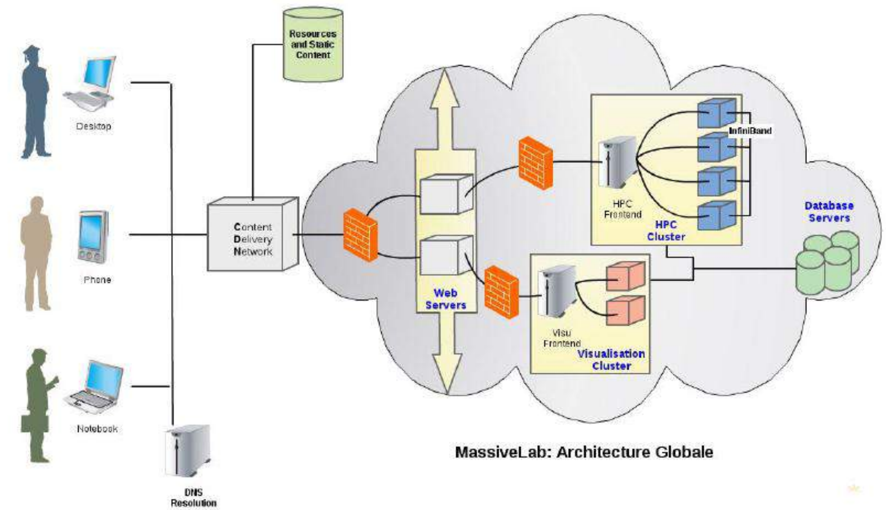

- ❑ Advantages of cloud computing:
  - →Less deployment
  - →High productivity
  - →Shared resources
  - →Environment friendly
  - →...*cloud-based solver and methods*

Mines ParisTech: Sophia Antipolis
Model name: Intel(R) Xeon(R) CPU E5-2640 0 @ 2.50GHz
~200 cores - 16 nodes (12 cores/nodes)

AEROMINES

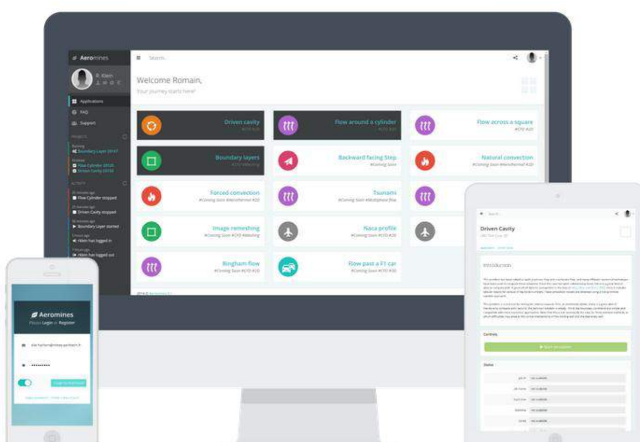

Context

❑ Advantages of cloud computing:

→Less deployment

→High productivity

→Shared resources

→Environment friendly

→… *cloud-based solver and methods*

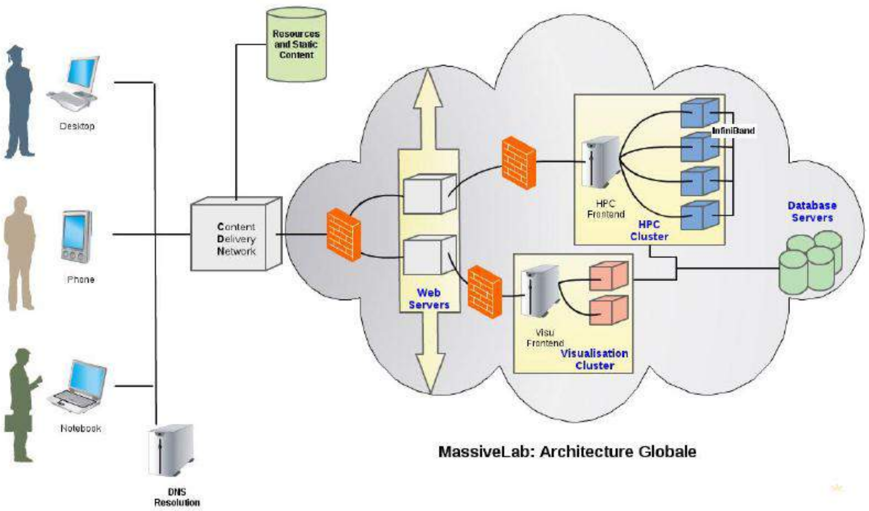

❑ Adaptive methods

→Immersed volume method (nurbs, complex geometries…)

→Space-Time anisotropic mesh adaptation (boundary layers, …)

→Customized applications

❑ Real world applications (3D, HPC)

→Fluid Structure Interaction solver

→Variational multiscale method for turbulent flows

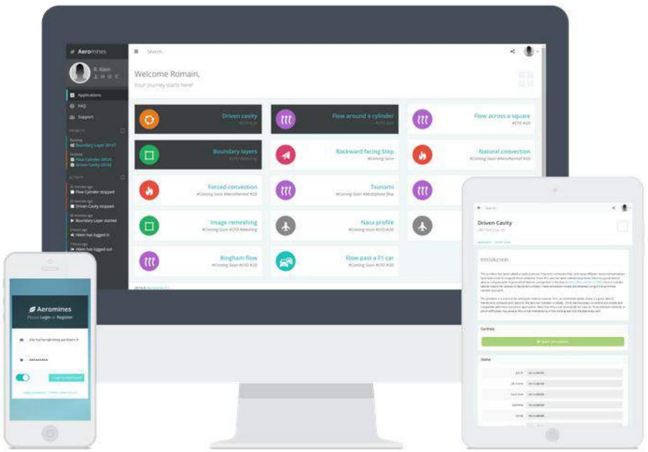

Illustrative example

3D Cooling using forced convection of an ingot at 1160° C placed on a grid inside a complex cavity

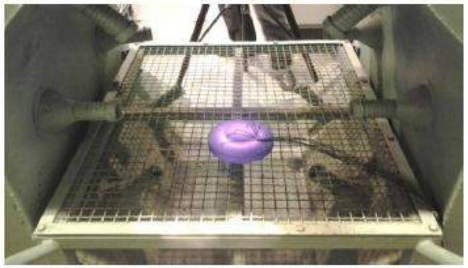

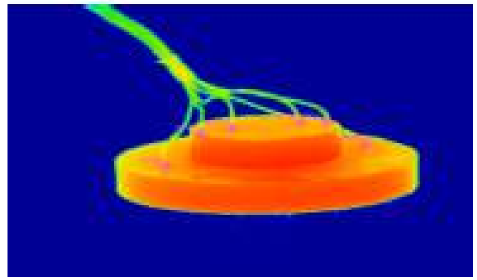

Snecma
Groupe SAFRAN

- -Natural convection in 3D
- -Radiative heat transfer (P1 model)
- -Initial temperature 1160° C
- -Navier-Stokes, RANS, Heat Trasnfer

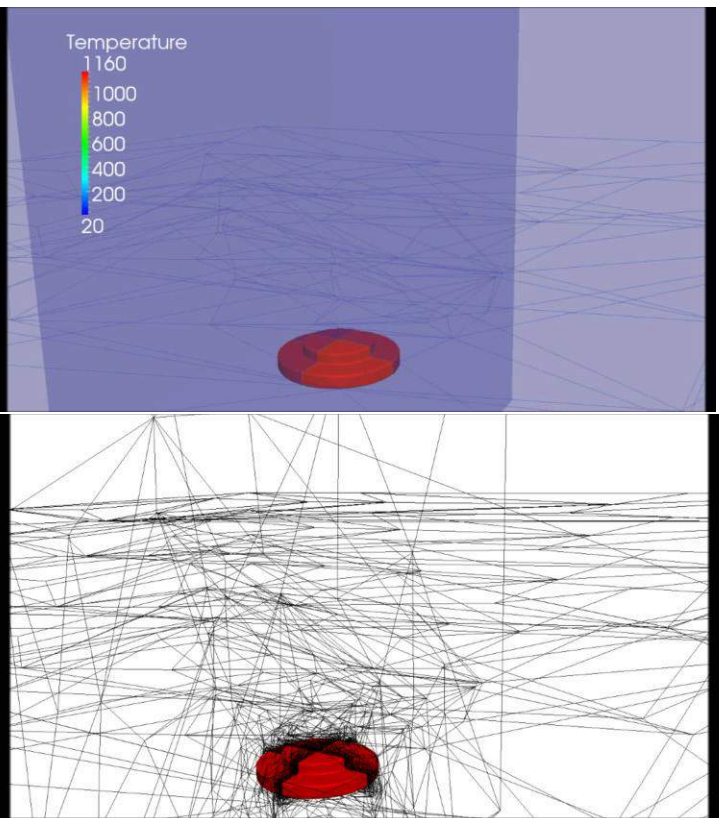

Direct numerical simulation

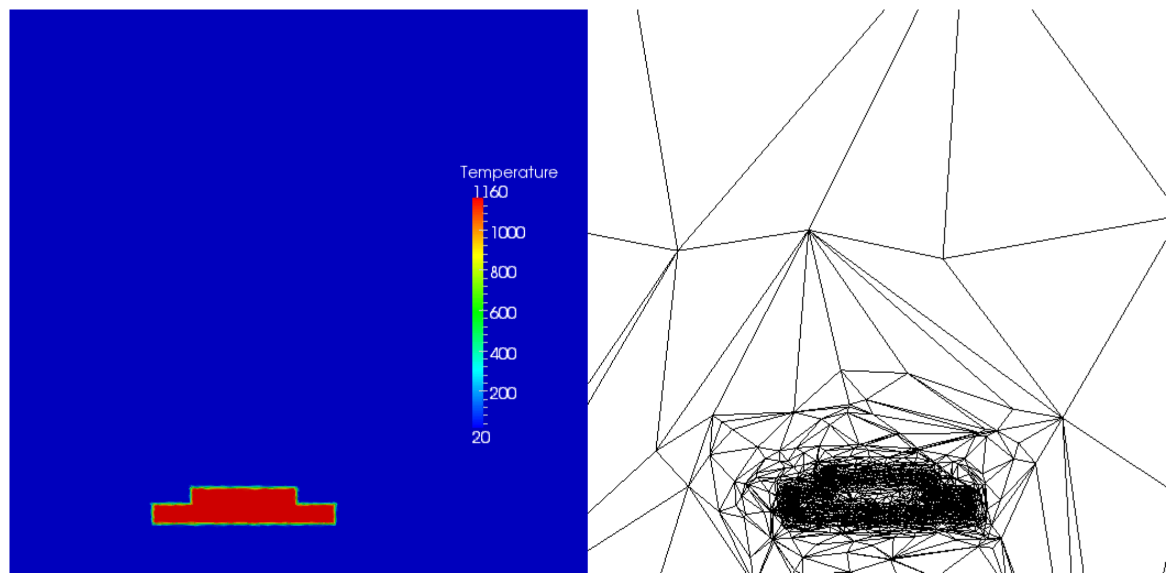

Adaptive Methods for Complex CFD problems:

Unsteady Navier-Stokes

Robust solver to handle high gradients and scale heterogeneities

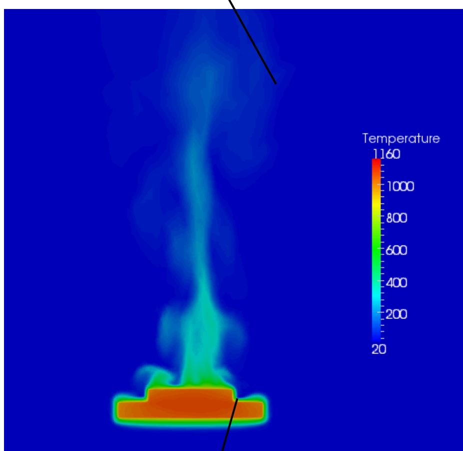

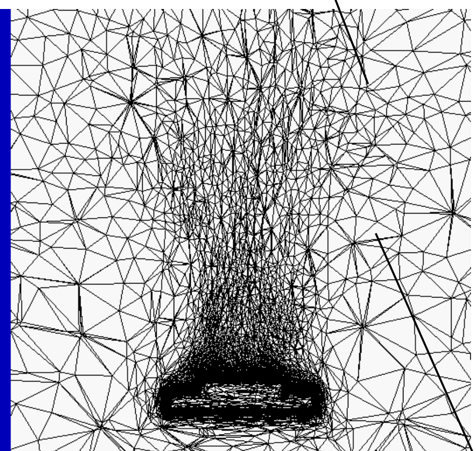

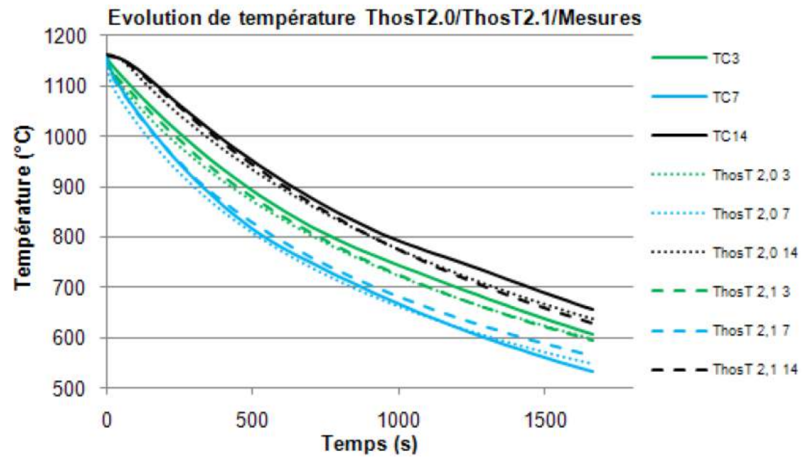

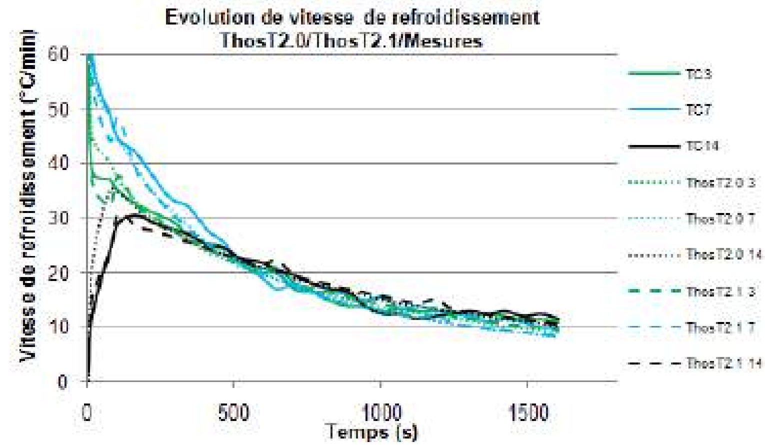

-Conjugate heat transfer
-Multidomain and immersed method
-No need for heat transfer coefficients

Multi criteria dynamic parallel anisotropic mesh adaptation

Immersed methods are well adapted for cloud computing

Immersed Stress Method

- ❑ Natural extension of the immersed volume method to deal with real FSI
- ❑ The desire to easily deal with large diversity of shapes and physical properties
- ❑ Make use of the developed flow solver

Classical Approaches

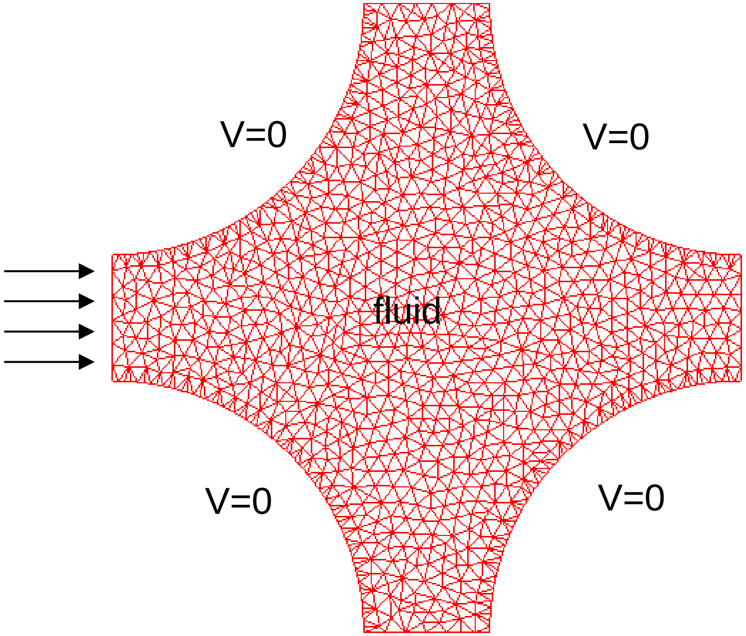

Immersed volume method

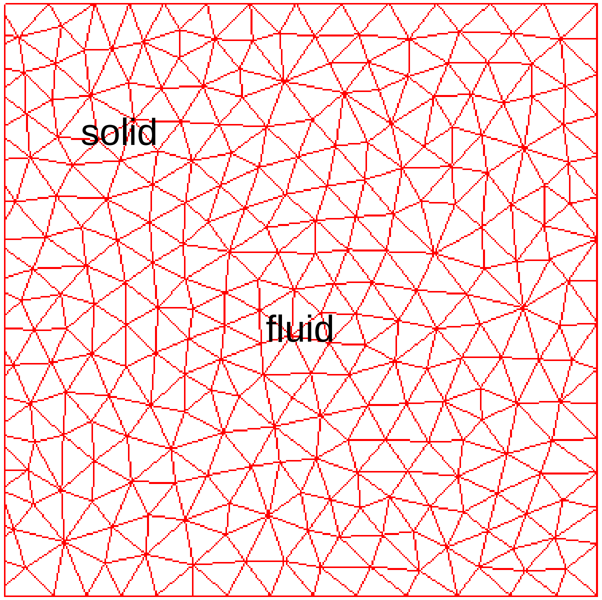

Levelset representation + Anisotropic Mesh adaptation

Immersed methods are well adapted for cloud computing

Immersed Stress Method

- ❑ Natural extension of the immersed volume method to deal with real FSI
- ❑ The desire to easily deal with large diversity of shapes and physical properties
- ❑ Make use of the developed flow solver

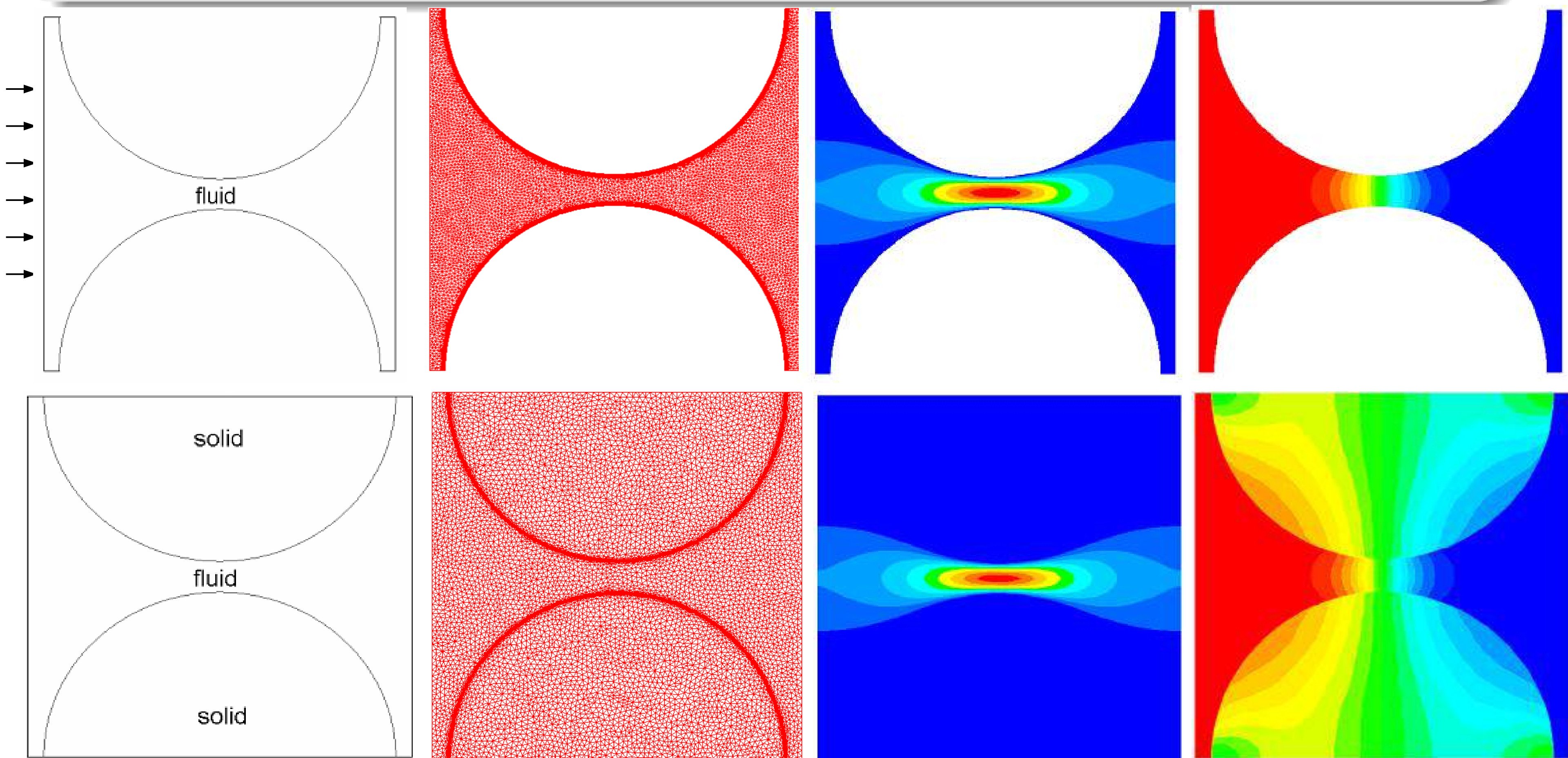

Immersed methods

Geomteric Representation

- ❑ Computing the distance function: **analytical** - surface mesh STL - NURBS iges
- ❑ LevelSet: sign the distance function
- ❑ Regularize it over a certain thickness and use it to mix the physical properties

$$\alpha(\mathbf{x}) = \pm d(\mathbf{x}, \Gamma_{\mathrm{im}}), \mathbf{x} \in \Omega,$$
$$\Gamma_{\mathrm{im}} = \{\mathbf{x}, \alpha(\mathbf{x}) = 0\}.$$

$$H_\varepsilon(\alpha) = \begin{cases} 1 & \text{if } \alpha > \varepsilon \\ \frac{1}{2}\left(1 + \frac{\alpha}{\varepsilon} + \frac{1}{\pi}\sin\left(\frac{\pi\alpha}{\varepsilon}\right)\right) & \text{if } |\alpha| \leq \varepsilon \\ 0 & \text{if } \alpha < -\varepsilon \end{cases}$$

$$\rho = \rho_f H(\alpha) + \rho_s(1 - H(\alpha))$$
$$\mu = \mu_f H(\alpha) + \mu_s(1 - H(\alpha))$$
$$\lambda = \left(\frac{H(\alpha)}{\lambda_f} + \frac{1 - H(\alpha)}{\lambda_s}\right)^{-1}$$

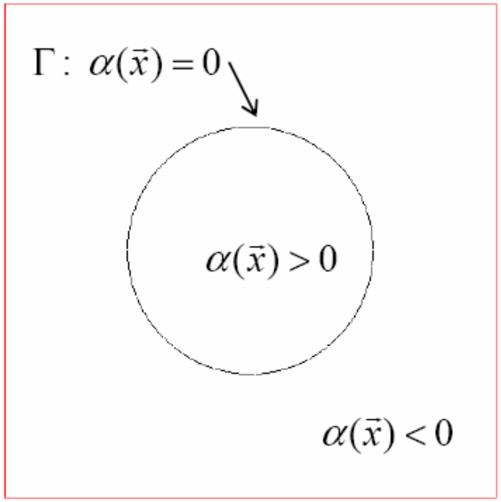

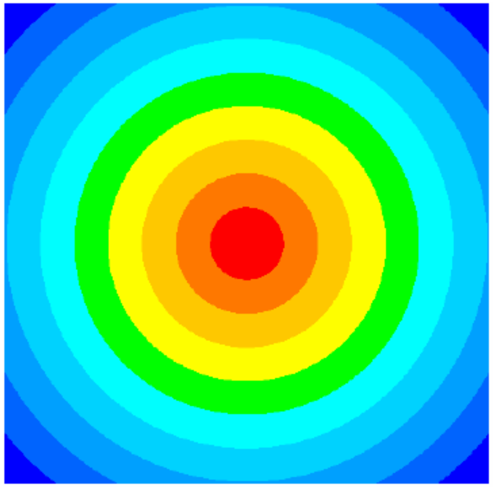

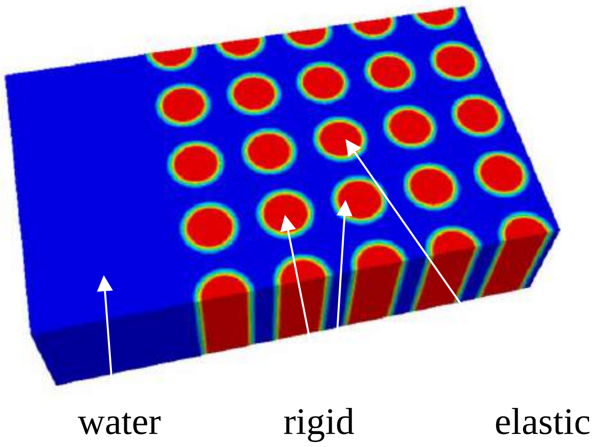

Immersed methods

Geomteric Representation

❑ Computing the distance function: analytical - surface mesh STL - NURBS iges

☒ The quality is limited by the given surface mesh

☒The cost can increase drastically

Helicopter.stl

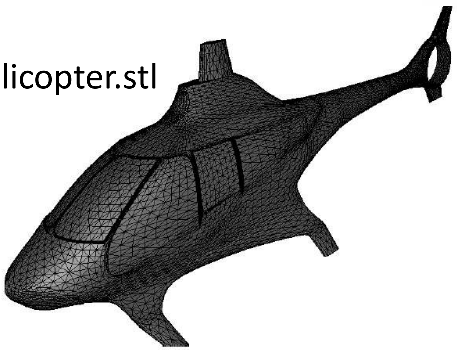

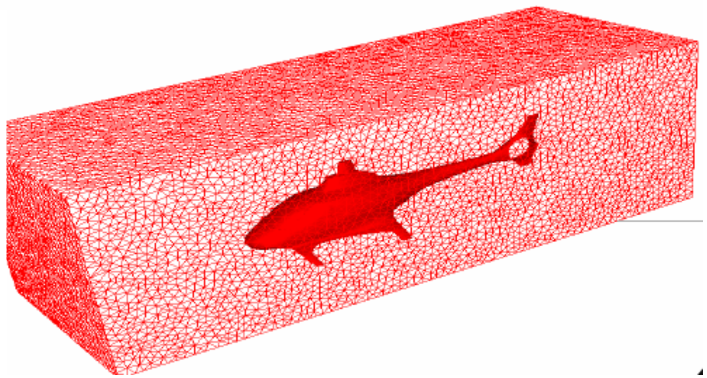

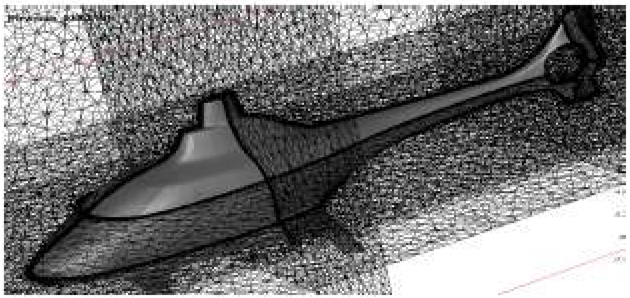

Iso-value zero of the levelset

The obtained mesh

Vehicule.stl

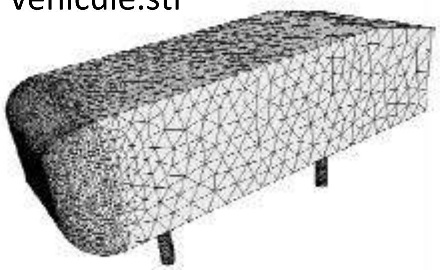

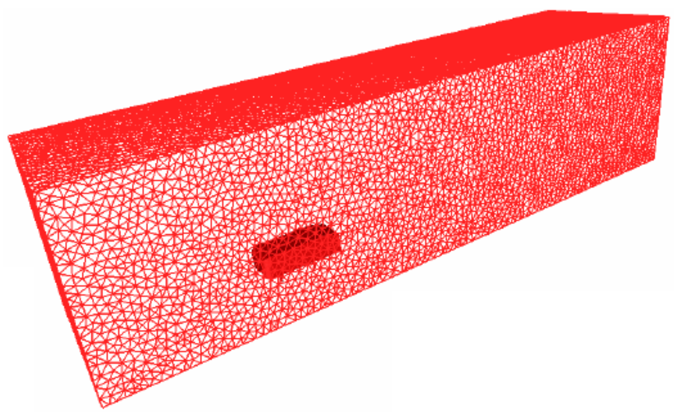

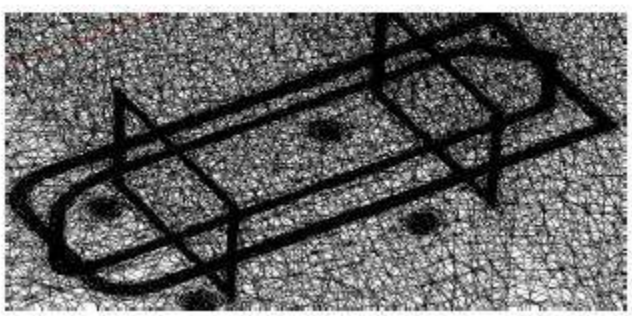

Immersed NURBS

New Geomteric Representation

- ❑ Computing the distance function: analytical - surface mesh STL - NURBS iges
- ✓ Bypass the generation of the surface mesh
- ✓ Increase the quality

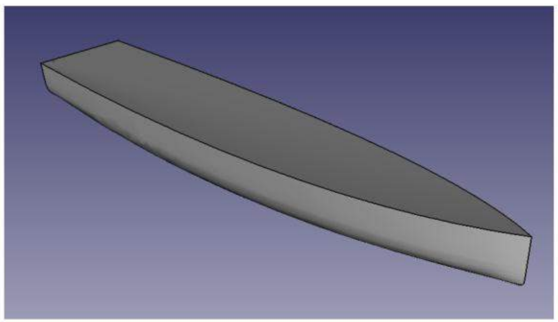

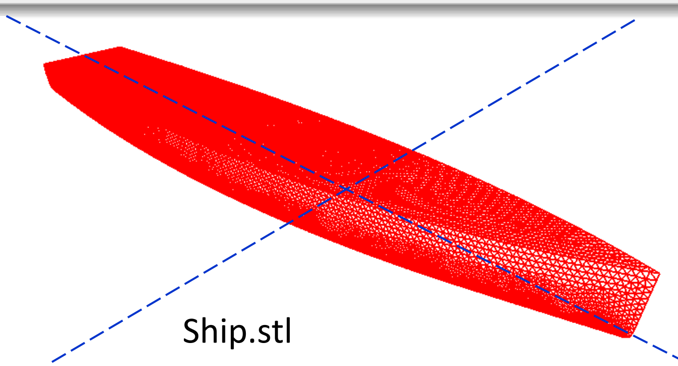

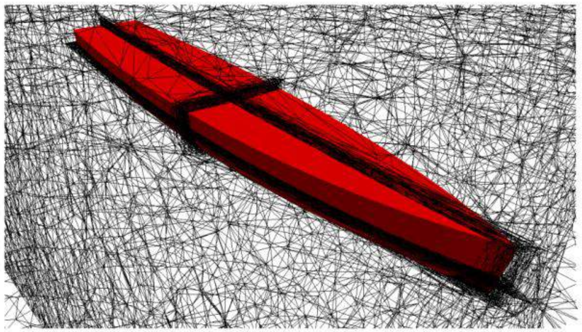

$$C(u)=\frac{\sum_{i=1}^{n} N_{i,p}(u).\omega_i .P_i}{\sum_{i=1}^{n} N_{i,p}(u).\omega_i}$$

$\longrightarrow$

Closest Point Problem:

$$(P-c(u^*)).c'(u^*)=0$$

$\longrightarrow$

Rational Bezier segments:

$$c(u)=\frac{\sum_{i=1}^{p} B_{i,p}(u)\omega_i P_i}{\sum_{i=1}^{p} B_{i,p}(u)\omega_i}$$

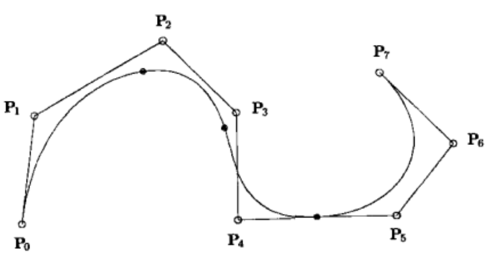

L.A. Piegl et W. Tiller, 1996

Newton method:

$$u_{i+1}=u_i-\frac{(c(u_i)-P).c'(u_i)}{(c(u_i-P).c''(u_i)+\|c'(u_i)\|^2}$$

p is the degree of the curve, Ni,p the basis functions, Pi the control points

Immersed NURBS

New Geomteric Representation [Phd J. Veysset 2011-2014]

- ❑ Computing the distance function: analytical - surface mesh STL - NURBS iges
- ✓ Bypass the generation of the surface mesh
- ✓ Increase the quality

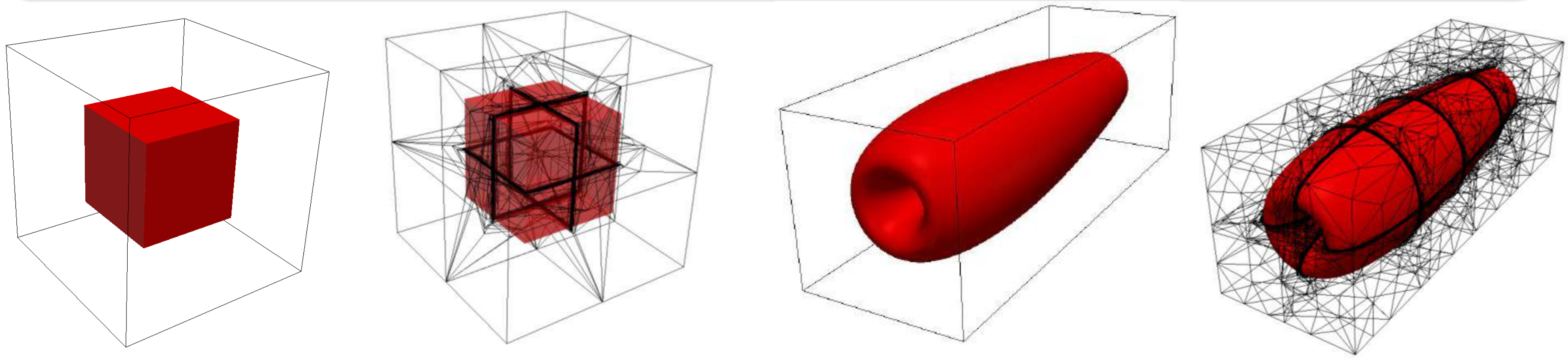

J. Veysset, E. Hachem, G. Jannoun, T. Coupez, *Immersed NURBS for CFD Applications*, SEMA SIMAI Springer Series, 2014

ncores	NURBS	Surface Mesh	NURBS + Transport
1	138.10	13.37	2.72
2	70.92	6.99	2.23
4	43.14	3.53	2.12
8	22.30	2.03	0.70

*E. Dyllong and W. Luther. Distance calculation between a point and a nurbs surface. In **Curve and Surface Design**, Saint-Malo, 55-62, 1999.*

*Y.L. Ma and W.T. Hewitt. Point inversion and projection for nurbs curve and surface: Control polygon approach. **Computer Aided Geometric Design**, 20:79–99, 2003.*

*E. Cohen and D. Johnson. Distance extrema for spline models using tangent cones. In **Proceedings of the Graphics Interface** 2005 Conference, May 9-11, 2005, Victoria, British Columbia, Canada, pages 169–175, 2005.*

Mesh Adaptation

Anisotropic Mesh Adaptation

- ❑ Enables to capture scale heterogeneities
- ❑ Enable to deal with discontinuities or gradients of the solution
- ❑ Important for boundary layers, shock waves, edge singularities
- ❑ Alternative to body-fitted mesh for very complex geometry: curvature, sharp angles,…

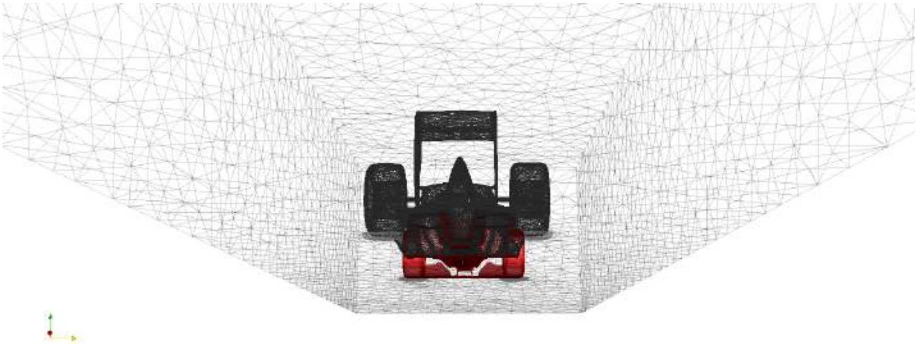

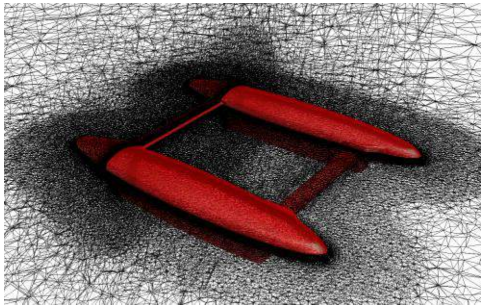

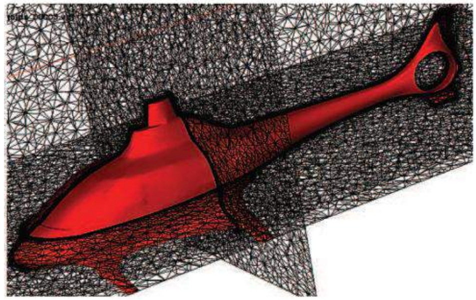

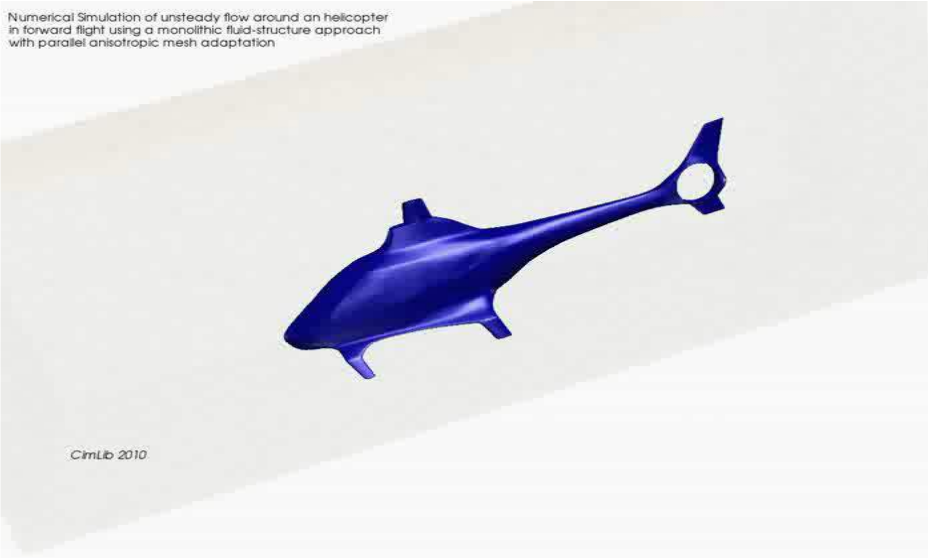

Dynamic Anisotropic Mesh Adaptation

Velocity: 300km/h
Number of nodes: 2 millions
Numer of cores: 96

Improvements

- ✓ Dynamic Mesh adaptation
- ✓ A posteriori error estimator
- ✓ Multi criteria adaptation
- ✓ Control (i.e. number of elements)
- ✓ Error analysis

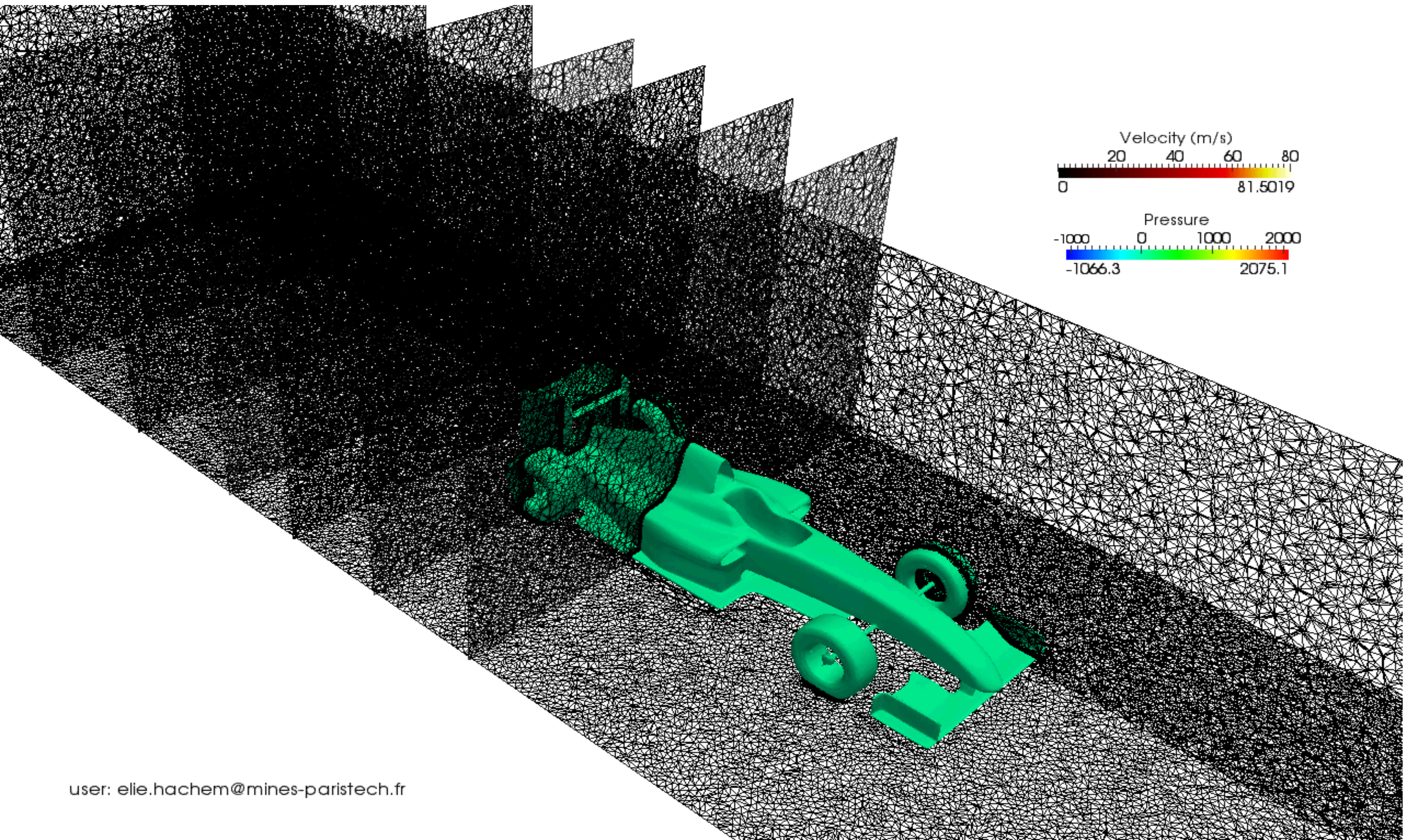

Space-Time Anisotropic Mesh Adaptation

From front to rear

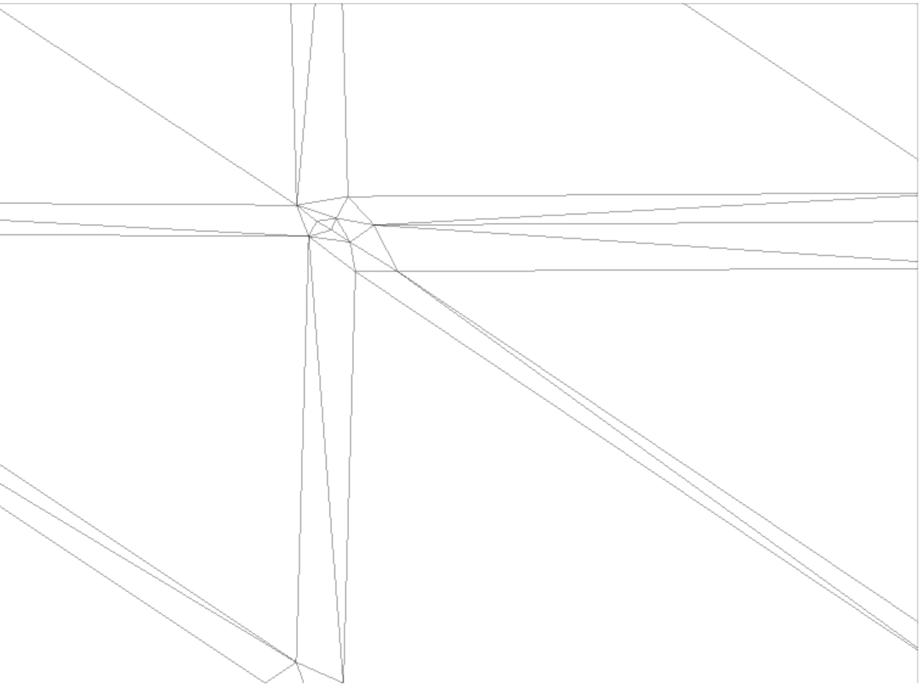

From buttom to top

Space-Time Anisotropic Mesh Adaptation

Candidate for directions:

$$\mathbb{X}^i = \frac{d}{|\Gamma(i)|} \sum_{j \in \Gamma(i)} \mathbf{X}^{ij} \otimes \mathbf{X}^{ij}$$

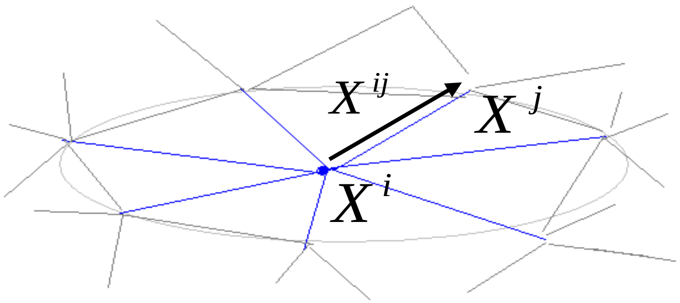

Control the size of each edge X^{ij} using a stretching factor:

$$\widetilde{\mathbf{X}^{ij}} = s_{ij} \mathbf{X}^{ij}$$

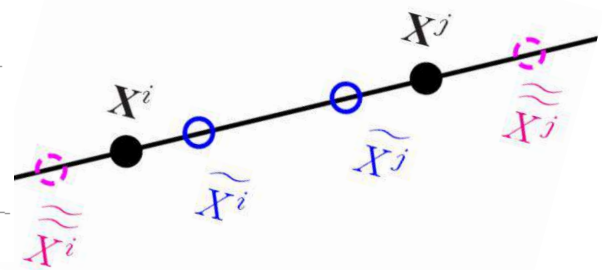

Drive these stretching factors using an edge based error estimator:

$$s_{ij} = \left(\frac{e}{e(N)}\right)^{-\frac{1}{2}} = \left(\frac{\sum_i n^i(1)}{N}\right)^{\frac{2}{d}} e_{ij}^{-1/2}$$

$$\boxed{\widetilde{\mathbb{M}}^i = \frac{|\Gamma(i)|}{d} \left(\widetilde{\mathbb{X}^i}\right)^{-1}}$$

Adaptive Time stepping

$$\tau_{n-1}^i = \left(\frac{e(N, t^n)/f}{e_i^{n,n-1}}\right)^{\frac{1}{2}}$$

$$\widetilde{\Delta t^n} = \min_i \tau_i^{n-1} \Delta t^n$$

E. Hachem, S. Feghali, R. Codina and T. Coupez, **Anisotropic Adaptive Meshing** and Monolithic Variational Multiscale Method for Fluid-Structure Interaction, Computer and Structures, Vol. 122, pp. 88 - 100, 2013

E. Hachem, G. Jannoun, J. Veysset, T. Coupez, On the stabilized finite element method for steady convection-dominated problems with **anisotropic mesh adaptation**, Applied Mathematics & Computation, Vol. 232, pp. 581-594, 2014

T. Coupez and E. Hachem, Solution of High-Reynolds Incompressible Flow with Stabilized Finite Element and **Adaptive Anisotropic Meshing**, Computer Methods in Applied Mechanics and Engineering, Vol. 267, pp. 65-85, 2013

Monolithic formulation for fluid structure interaction

Immersed Stress Method

$$\rho\,(\partial_t \mathbf{v} + \mathbf{v}\cdot\nabla\mathbf{v}) - \nabla\cdot(2\eta\,\varepsilon(\mathbf{v}) + \boldsymbol{\tau} - p\,\mathbf{I}_d) = \mathbf{f} \qquad \text{in } \Omega,\ t>0$$

$$\nabla\cdot\mathbf{v} = 0 \qquad \text{in } \Omega,\ t>0$$

E. Hachem, S. Feghali, R. Codina and T. Coupez, Immersed Stress Method for Fluid Structure Interaction, submitted to International Journal for Numerical Methods in Engineering, 2012

$$\boldsymbol{\sigma} = \boldsymbol{\tau}_{\mathrm{s}} - p\,\mathbf{I}_d$$

$$\boldsymbol{\sigma} = 2\eta_{\mathrm{f}}\,\varepsilon(\mathbf{v}) - p\,\mathbf{I}_d$$

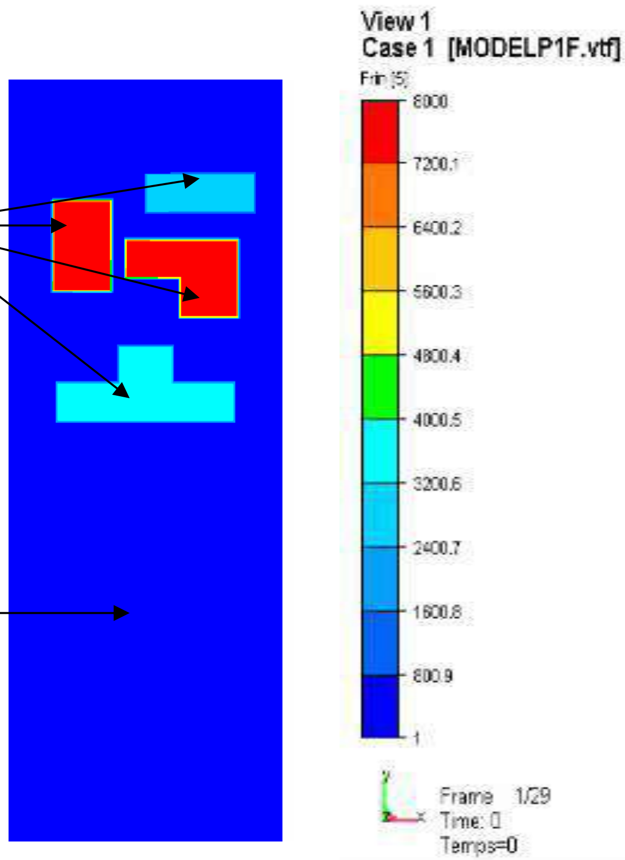

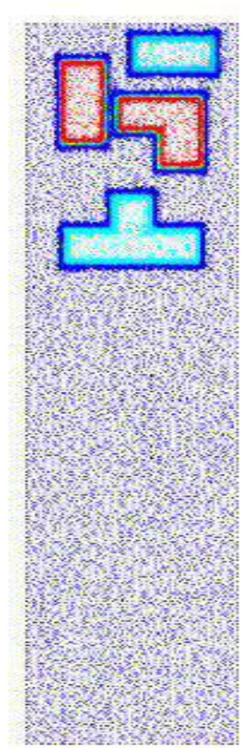

Monolithic formulation for fluid structure interaction

Immersed Stress Method

$$\rho\,(\partial_t \mathbf{v} + \mathbf{v}\cdot\nabla\mathbf{v}) - \nabla\cdot(2\eta\,\varepsilon(\mathbf{v}) + \boldsymbol{\tau} - p\,\mathbf{I}_d) = \mathbf{f} \qquad \text{in } \Omega,\ t>0$$

$$\nabla\cdot\mathbf{v} = 0 \qquad \text{in } \Omega,\ t>0$$

E. Hachem, S. Feghali, R. Codina and T. Coupez, Immersed Stress Method for Fluid Structure Interaction, submitted to International Journal for Numerical Methods in Engineering, 2012

$$\boldsymbol{\sigma}_s = \tfrac{2}{3}E\varepsilon(\mathbf{u}) - p\,\mathbf{I_d}$$

$$\boldsymbol{\sigma} = 2\eta_{\mathrm{f}}\ \varepsilon(\mathbf{v}) - p\,\mathbf{I}_d$$

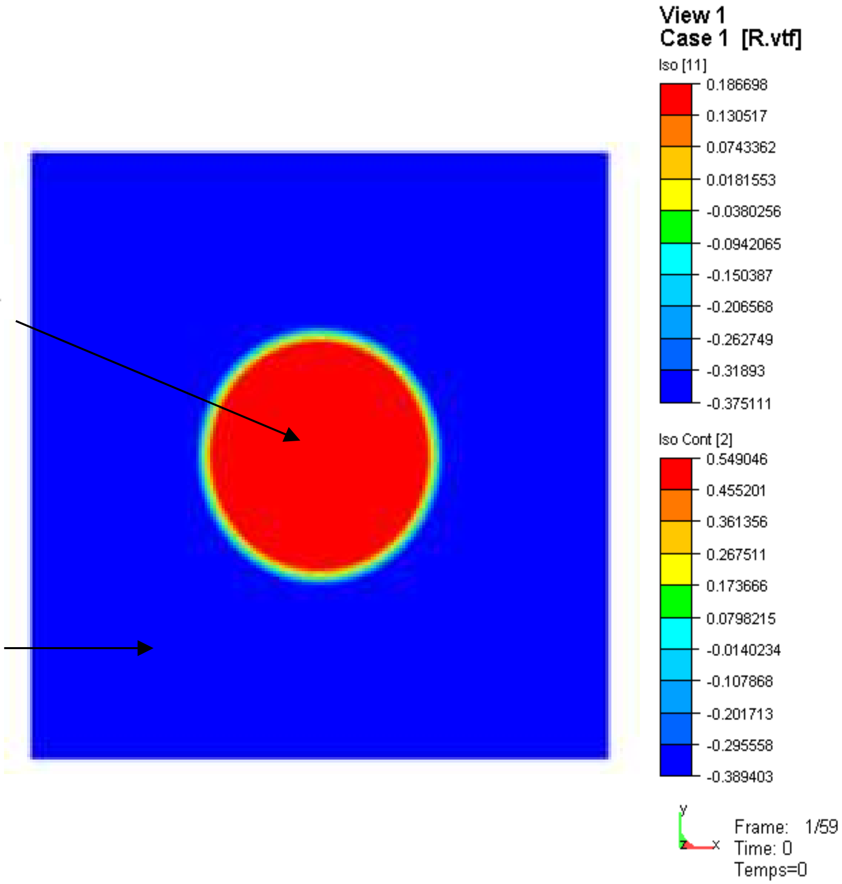

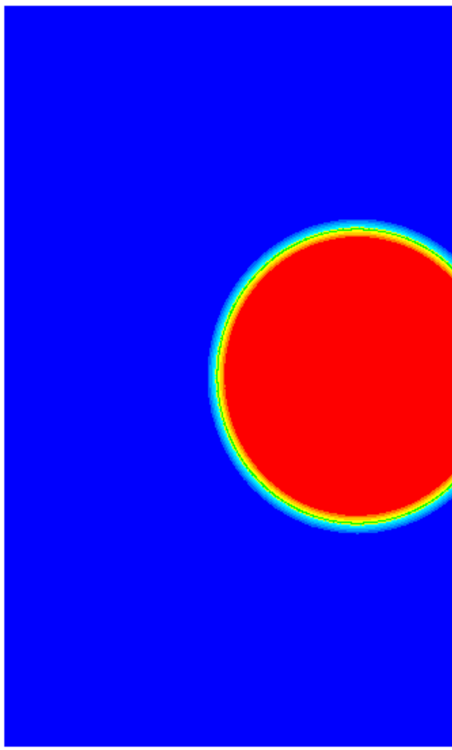

Three-field SFEM for fluid-structure interaction

Variational Multiscale Method:

Let us split the velocity, pressure and stress solution spaces as $V_h \oplus V'$, $P_h \oplus P'$ and $\mathcal{T}_h \oplus \mathcal{T}'$, respectively

$$
\begin{aligned}
\mathbf{v} &= \mathbf{v}_h + \mathbf{v}' \in V_h \oplus V' \\
p &= p_h + p' \in P_h \oplus P' \\
\boldsymbol{\tau} &= \boldsymbol{\tau}_h + \boldsymbol{\tau}' \in \mathcal{T}_h \oplus \mathcal{T}'
\end{aligned}
$$

[Masud & Xia 2005]
[Cervera & Codina 2010]
[Hachem et al. 2010]

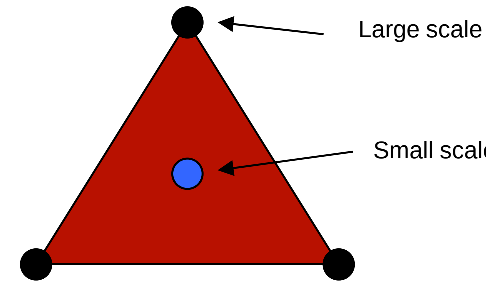

find $(\mathbf{v}_h + \mathbf{v}', p_h + p', \boldsymbol{\tau}_h + \boldsymbol{\tau}') \in V_h \oplus V' \times P_h \oplus P' \times \mathcal{T}_h \oplus \mathcal{T}'$ such that

$$
\begin{aligned}
\rho(\delta_t(\mathbf{v}_h + \mathbf{v}'), \mathbf{w}_h + \mathbf{w}') + \rho((\mathbf{v}_h + \mathbf{v}') \cdot \nabla(\mathbf{v}_h + \mathbf{v}'), \mathbf{w}_h + \mathbf{w}') - (p_h + p', \nabla \cdot (\mathbf{w}_h + \mathbf{w}')) \\
+ 2(\eta \varepsilon(\mathbf{v}_h + \mathbf{v}'), \varepsilon(\mathbf{w}_h + \mathbf{w}')) + (\boldsymbol{\tau}_h + \boldsymbol{\tau}', \varepsilon_{\mathrm{s}}(\mathbf{w}_h + \mathbf{w}')) = \langle \mathbf{f}, \mathbf{w}_h + \mathbf{w}' \rangle \\
(q_h + q', \nabla \cdot (\mathbf{v}_h + \mathbf{v}')) = 0 \\
-(\boldsymbol{\xi}_h + \boldsymbol{\xi}', \varepsilon_{\mathrm{s}}(\mathbf{v}_h + \mathbf{v}')) = 0
\end{aligned}
$$

The obtained coarse scale is given by:

$$
\begin{aligned}
\rho(\delta_t \mathbf{v}_h, \mathbf{w}_h) + \rho(\mathbf{v}_h \cdot \nabla \mathbf{v}_h, \mathbf{w}_h) - (p_h + p', \nabla \cdot \mathbf{w}_h) + 2(\eta \varepsilon(\mathbf{v}_h), \varepsilon(\mathbf{w}_h)) + (\boldsymbol{\tau}_h + \boldsymbol{\tau}', \varepsilon_{\mathrm{s}}(\mathbf{w}_h)) \\
+ \sum_K (\mathbf{v}', -\rho \mathbf{v}_h \cdot \nabla \mathbf{w}_h - \nabla \cdot (2\eta \varepsilon(\mathbf{w}_h)))_K = \langle \mathbf{f}, \mathbf{w}_h \rangle \\
(q_h, \nabla \cdot \mathbf{v}_h) - \sum_K (\mathbf{v}', \nabla q_h)_K = 0 \\
-(\varepsilon_{\mathrm{s}}(\mathbf{v}_h), \boldsymbol{\xi}_h) + \sum_K (\mathbf{v}', \chi_{\mathrm{s}} \nabla \cdot \boldsymbol{\xi}_h)_K = 0
\end{aligned}
$$

Fluid: high Reynolds number (implicit VMS-LES)
Structure rigid or elastic

The subscales may be approximated within each element K by:

$$\mathbf{v}' = \alpha_v \Pi'_v(\mathcal{R}_v), \quad p' = \alpha_p \Pi'_p(\mathcal{R}_p), \quad \boldsymbol{\tau}' = \alpha_\tau \Pi'_\tau(\mathcal{R}_\tau)$$

Inserting the expression for the subscales, we finally obtain the stabilized finite element problem:

$$\begin{aligned}
&\rho(\delta_t \mathbf{v}_h, \mathbf{w}_h) + \rho(\mathbf{v}_h \cdot \nabla \mathbf{v}_h, \mathbf{w}_h) - (p_h, \nabla \cdot \mathbf{w}_h) + 2(\eta \boldsymbol{\varepsilon}(\mathbf{v}_h), \boldsymbol{\varepsilon}(\mathbf{w}_h)) + (\boldsymbol{\tau}_h, \boldsymbol{\varepsilon}_{\mathrm{s}}(\mathbf{w}_h)) \\
&\quad + \sum_K \alpha_v (\rho \delta_t \mathbf{v}_h + \underline{\rho \mathbf{v}_h \cdot \nabla \mathbf{v}_h} + \nabla p_h - \chi_{\mathrm{s}} \nabla \cdot \boldsymbol{\tau}_h - \nabla \cdot (2\eta \boldsymbol{\varepsilon}(\mathbf{v}_h)), \underline{\rho \mathbf{v}_h \cdot \nabla \mathbf{w}_h} + \nabla \cdot (2\eta \boldsymbol{\varepsilon}(\mathbf{w}_h)))_K \\
&\quad + \sum_K \alpha_p (\nabla \cdot \mathbf{v}_h, \nabla \cdot \mathbf{w}_h) + \sum_K \alpha_\tau (\boldsymbol{\varepsilon}_{\mathrm{s}}(\mathbf{v}_h), \boldsymbol{\varepsilon}_{\mathrm{s}}(\mathbf{w}_h)) \\
&\quad = \langle \mathbf{f}, \mathbf{w}_h \rangle + \sum_K \alpha_v (\mathbf{f}, \rho \mathbf{v}_h \cdot \nabla \mathbf{w}_h + 2\eta \nabla \cdot \boldsymbol{\varepsilon}(\mathbf{w}_h))_K \\
&(q_h, \nabla \cdot \mathbf{v}_h) + \sum_K \alpha_v (\rho \delta_t \mathbf{v}_h + \rho \mathbf{v}_h \cdot \nabla \mathbf{v}_h + \nabla p_h - \chi_{\mathrm{s}} \nabla \cdot \boldsymbol{\tau}_h - \nabla \cdot (2\eta \boldsymbol{\varepsilon}(\mathbf{v}_h)), \nabla q_h)_K \\
&\quad = \sum_K \alpha_v (\mathbf{f}, \nabla q_h)_K \\
&-(\boldsymbol{\varepsilon}_{\mathrm{s}}(\mathbf{v}_h), \boldsymbol{\xi}_h) + \sum_K \alpha_v (\rho \delta_t \mathbf{v}_h + \rho \mathbf{v}_h \cdot \nabla \mathbf{v}_h + \nabla p_h - \chi_{\mathrm{s}} \nabla \cdot \boldsymbol{\tau}_h - \nabla \cdot (2\eta \boldsymbol{\varepsilon}(\mathbf{v}_h)), -\chi_{\mathrm{s}} \nabla \cdot \boldsymbol{\xi}_h)_K \\
&\quad = \sum_K \alpha_v (\mathbf{f}, -\chi_{\mathrm{s}} \nabla \cdot \boldsymbol{\xi}_h)_K
\end{aligned}$$

Combining anisotropic meshing and SFEM

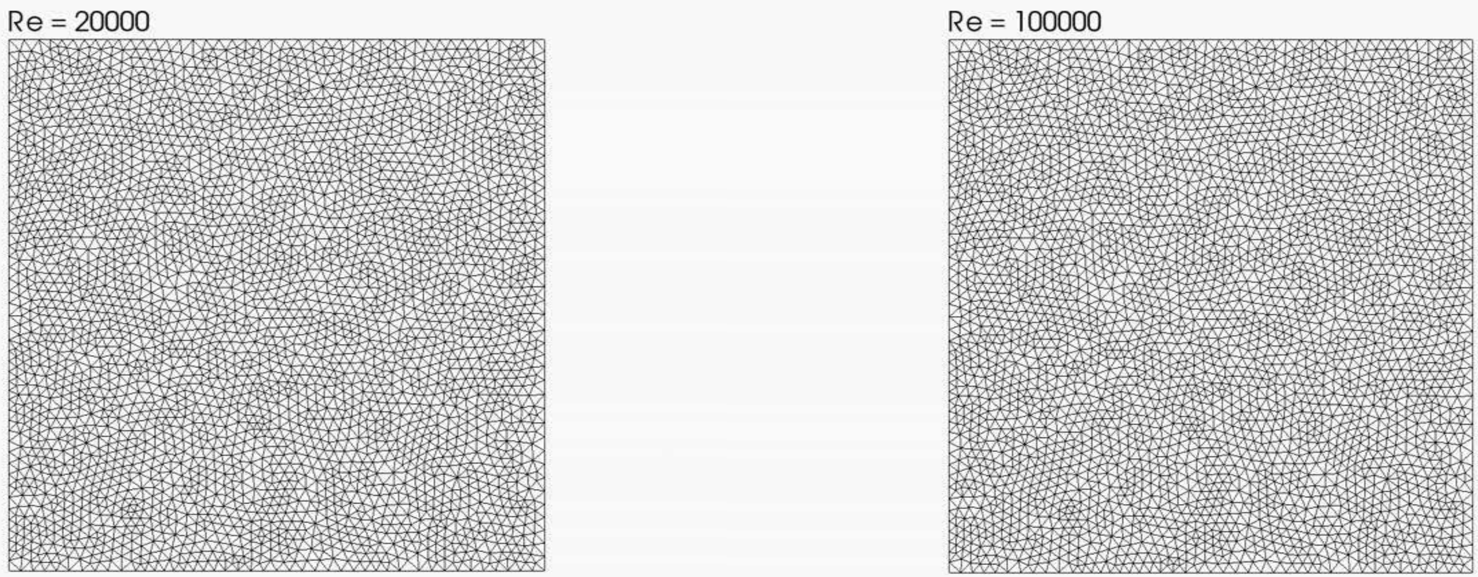

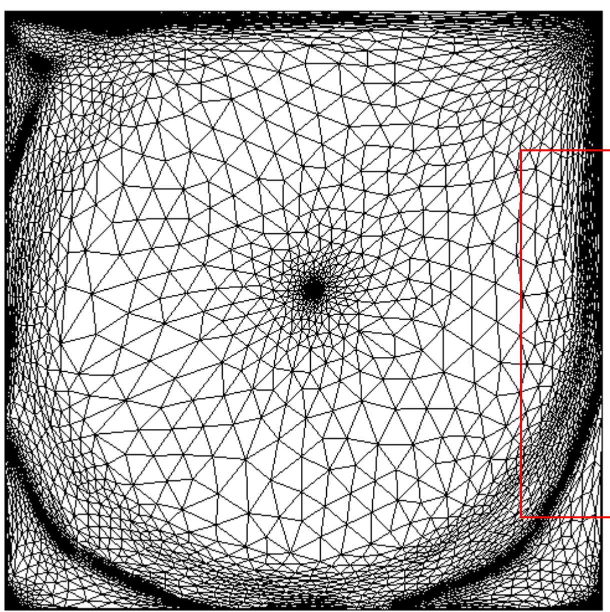

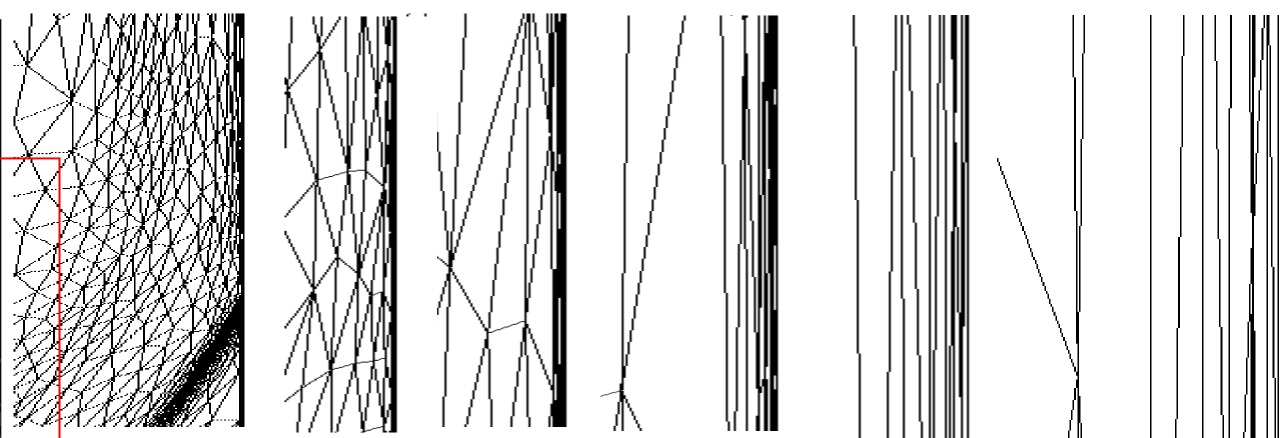

J. L. Guermond and P. D. Minev, Start-up flow in a three-dimensional lid-driven cavity by means of a massively parallel direction splitting algorithmInt. J. Numer. Meth. Fluids (**2011**)

New benchmark (tabulated results in 2D and 3D)

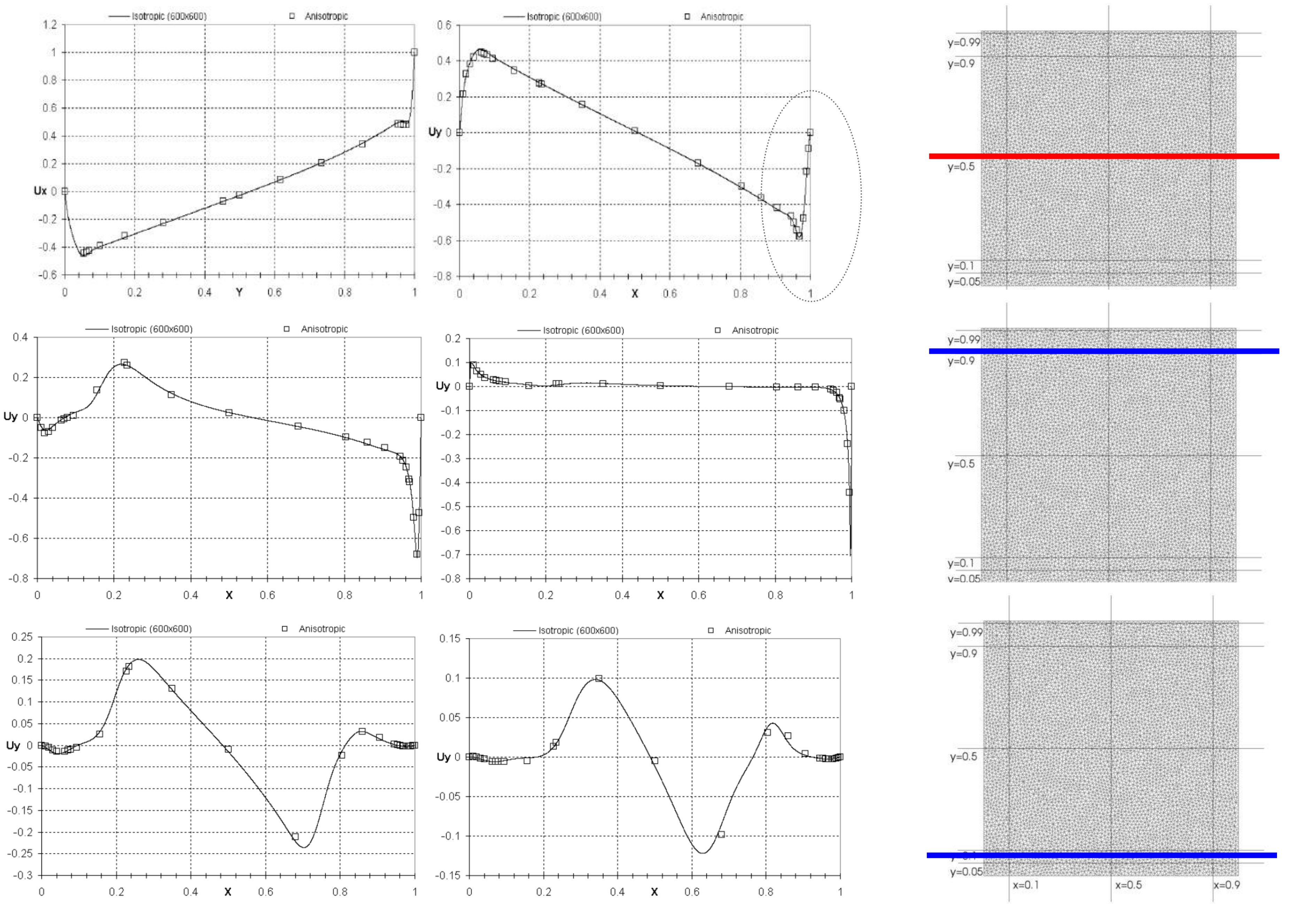

Numerical examples:

[Phd S. Feghali, 2011-2013]

Oscillating disk in a channel

Fictitious boundary and moving mesh methods for the numerical simulation of rigid particulate flows Decheng et al. 2007]

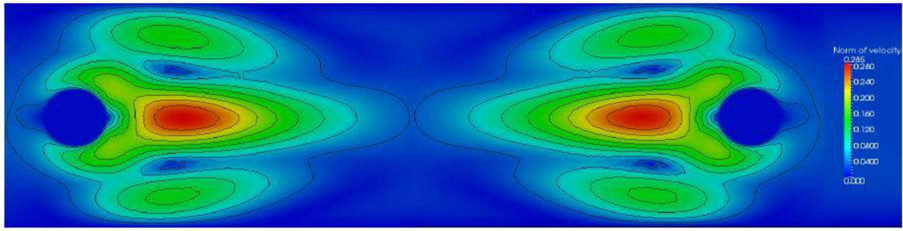

Norm of velocity at t=18.9s (left) and t=21s (right)

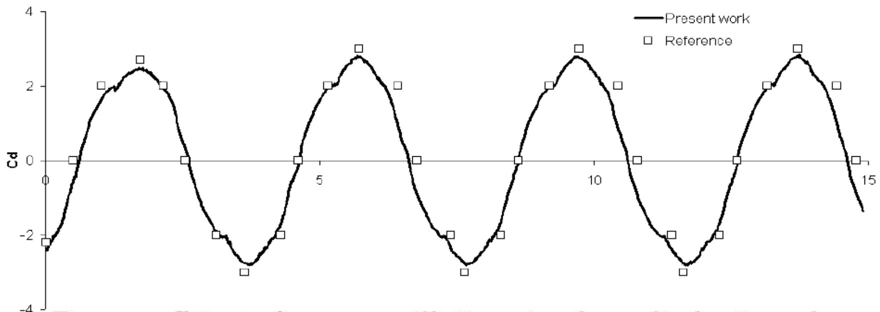

Drag coeffcients for one oscillating circular cylinder in a channel

Falling disk in a channel

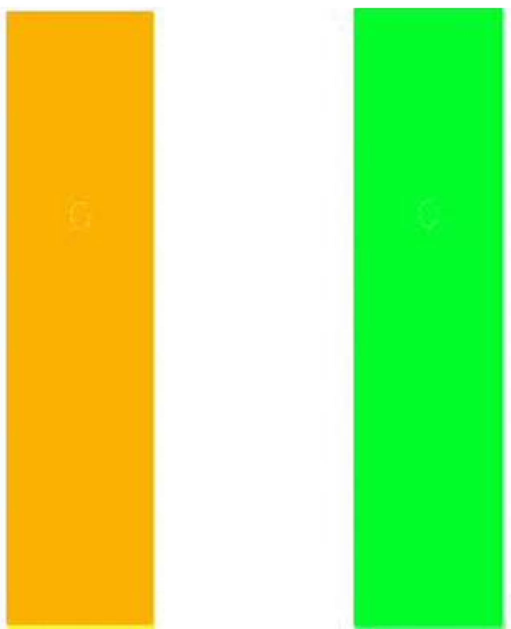

Table II. Terminal velocity for the falling cylinder problem.

η_f	Reference [47] 160×640	$h = 0.002$	$h = 0.001$	$h = 0.0005$	$h = 0.00025$	Convergence order
0.1	−0.1966	−0.1503069	−0.167770	−0.19230704	−0.196834	∼ 2.3
0.2	−0.1417	−0.10756319	−0.12367	−0.13596088	−0.14087306	∼ 1.8
0.5	−0.06721	−0.04301721	−0.0579240	−0.0645362	−0.066432	∼ 1.7

Robinson A, Schroeder C, Fedkiw R. A symmetric positive definite formulation for monolithic fluid structure interaction. Journal of Computational Physics 2010; 230(4):1547–1566.

Flow past a NACA0012 with VMS

	Fluent 23876 nodes	Presentwork 10000 nodes
Cd	0.0561	0.05577

Reynolds 5000

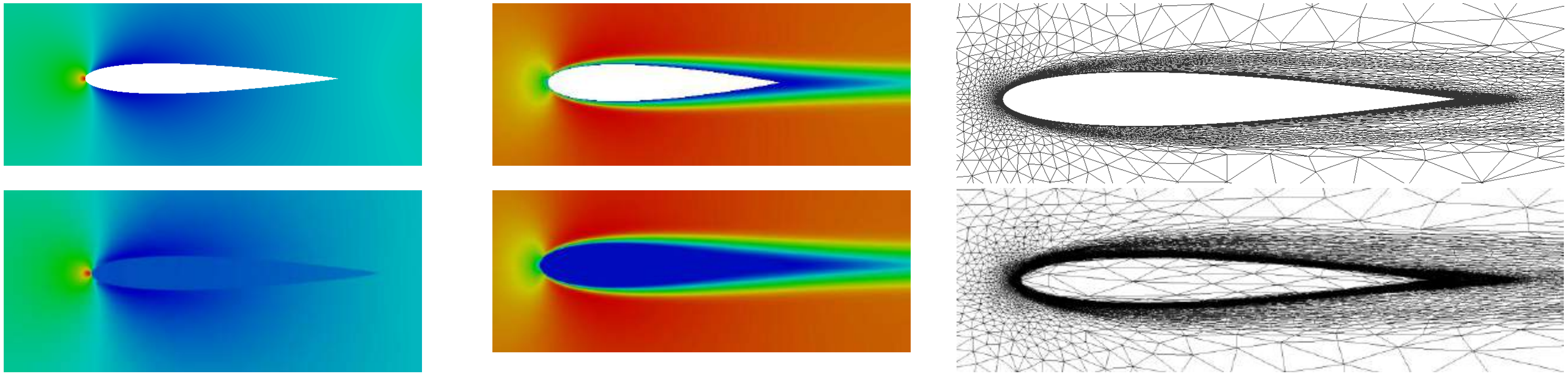

Reynolds 500000

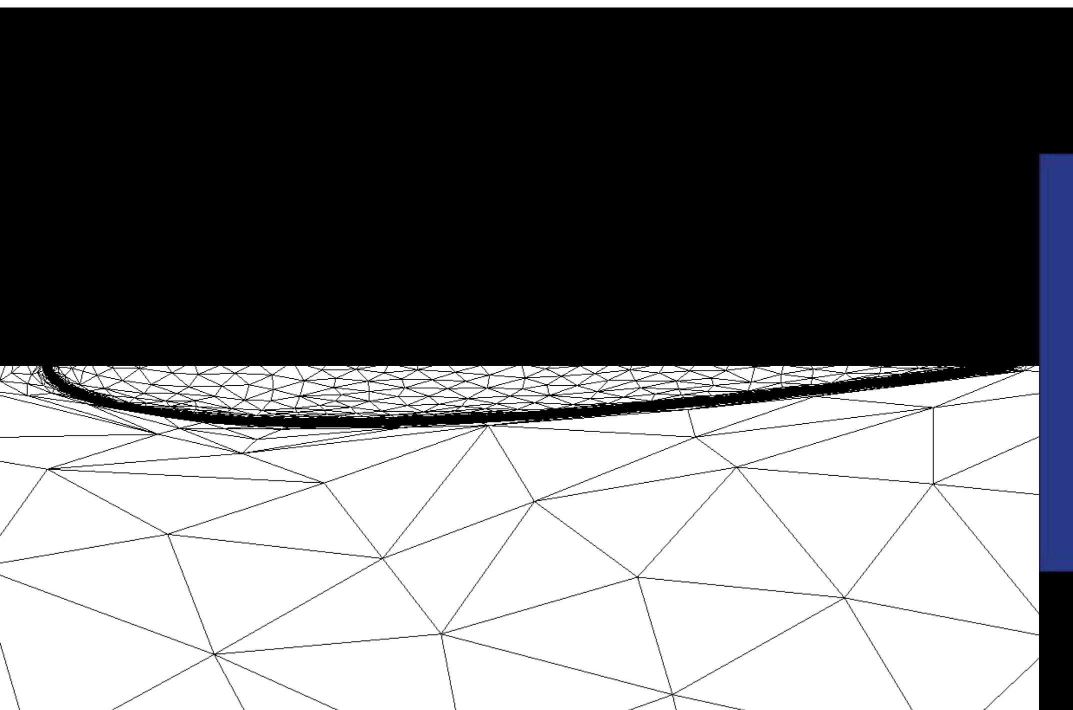

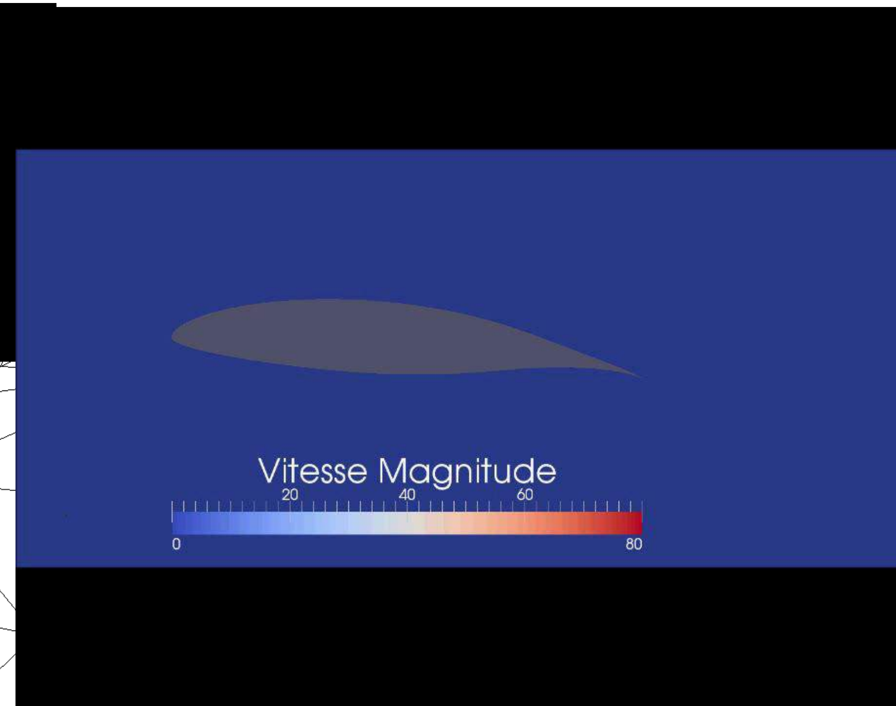

Turbulent flows past an immersed complex geometries

airship

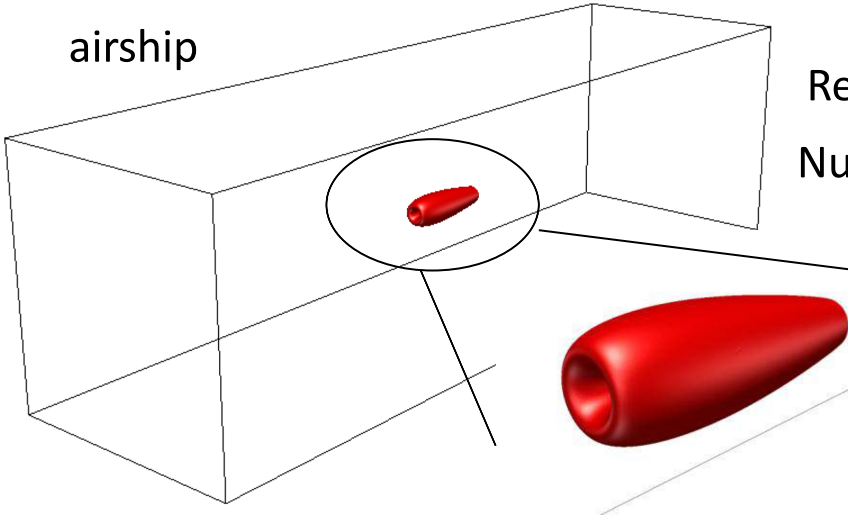

Reynolds number ~10^7

Number of elements ~2.10^6

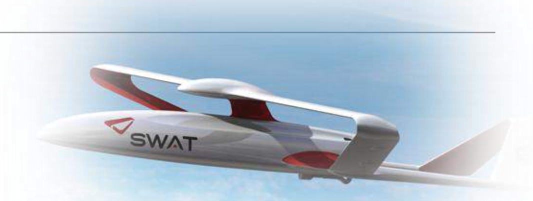

drone

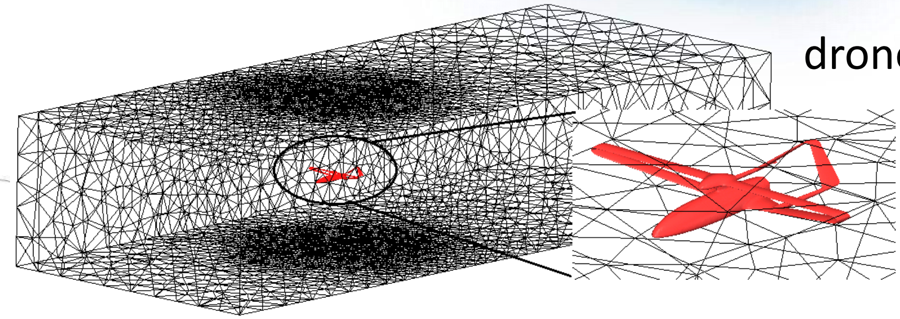

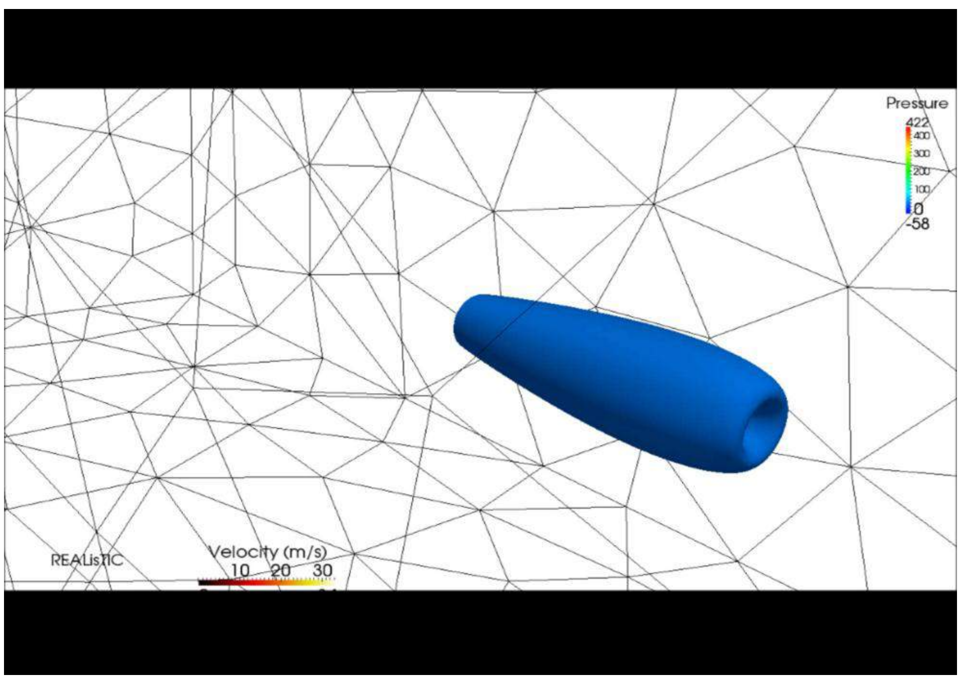

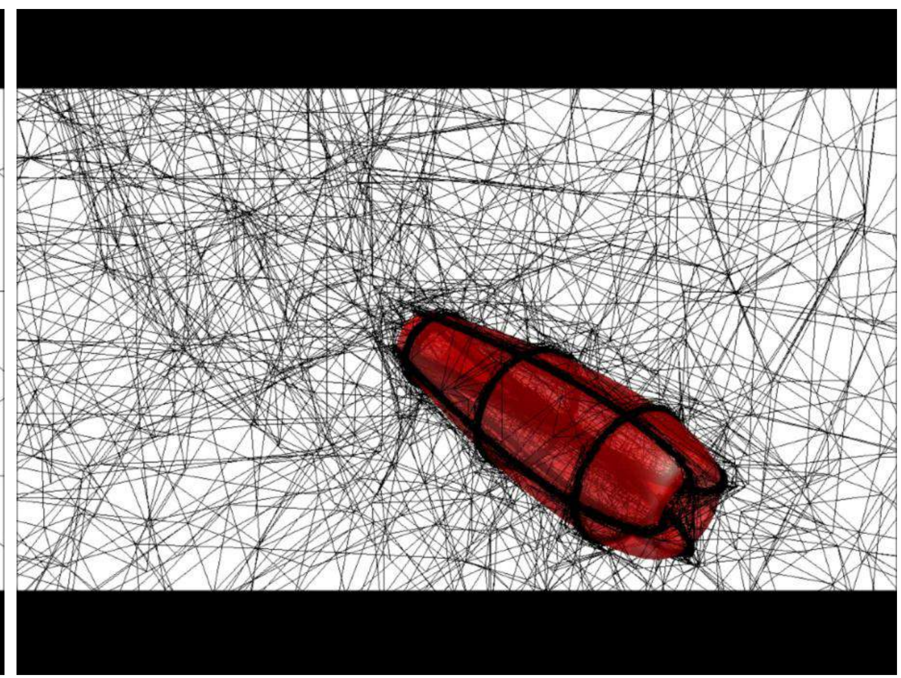

Turbulent flows past an immersed complex geometries

airship

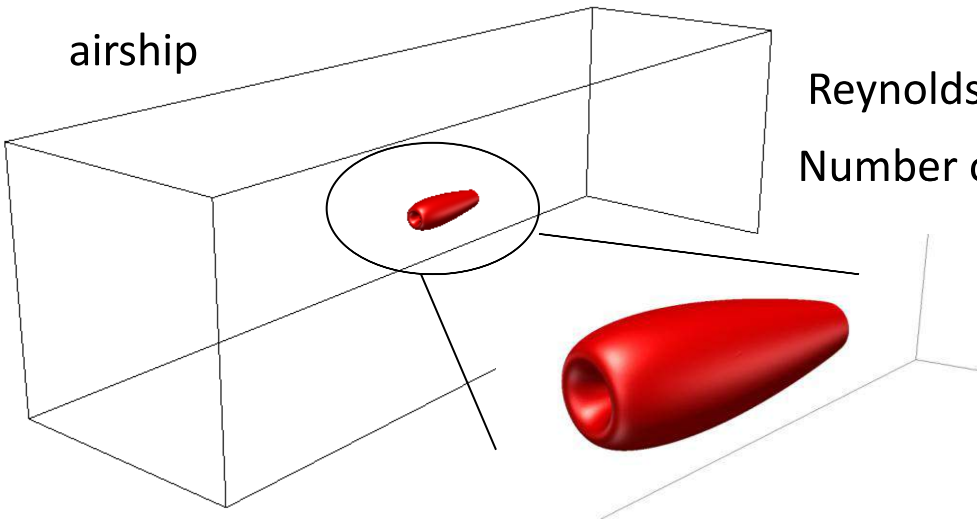

Reynolds number ~10^7

Number of elements ~2.10^6

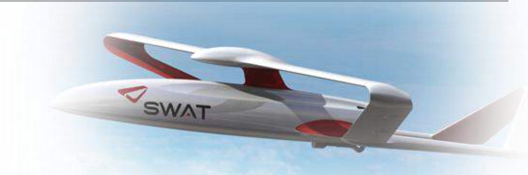

drone

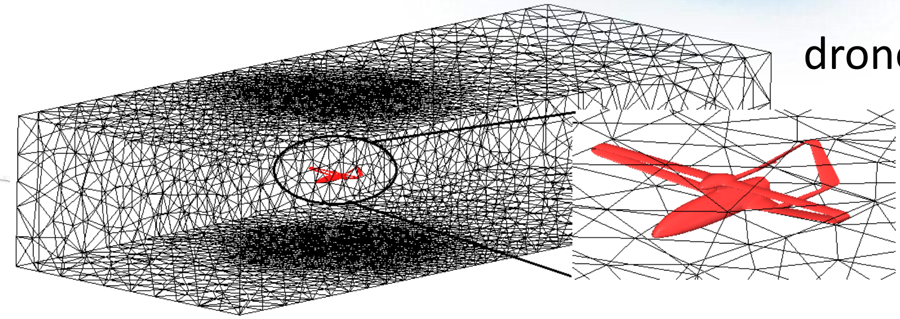

User parameters:
-Velocity
-Angle of attack

Solution:
-Drag
- Lift
- Pressure
- Velocity

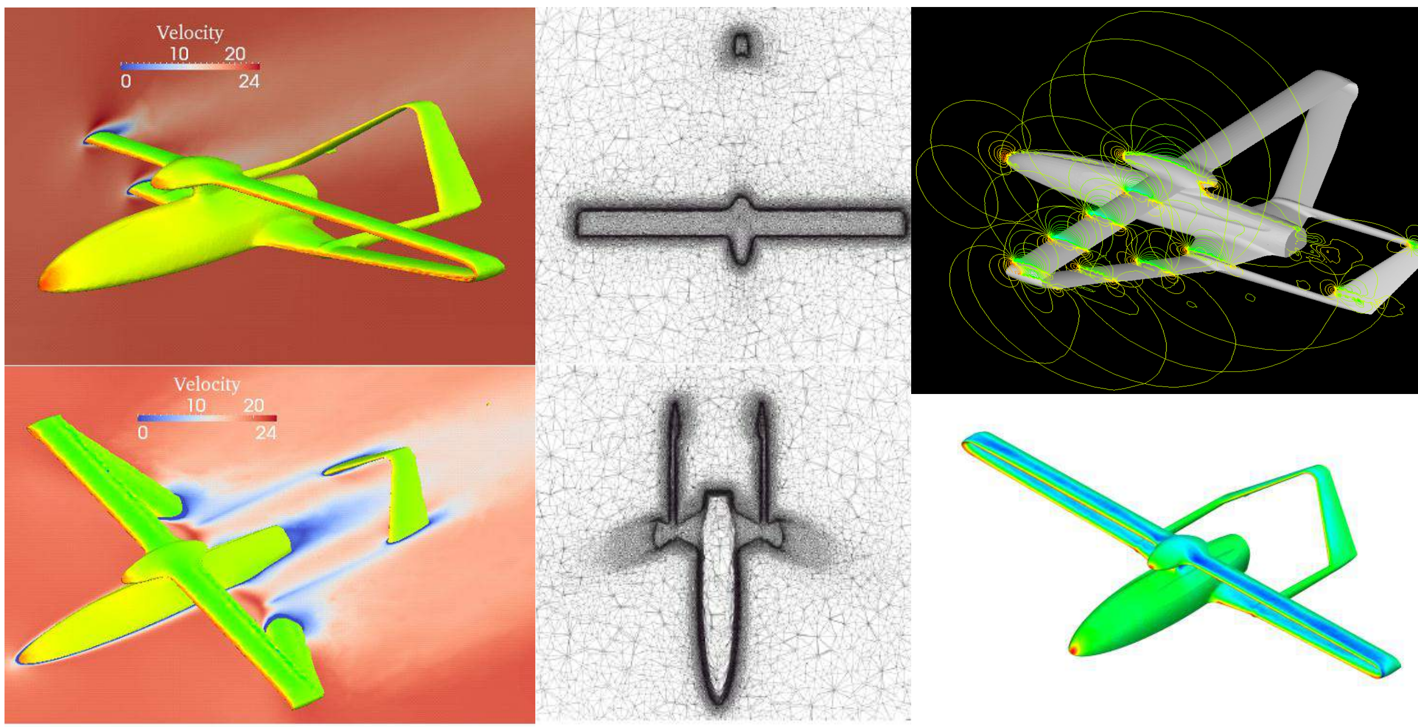

Parallel anisotropic adaptation with moving embedded geometries

A posteriori edge-based error estimator
Anisotropic Meshing with highly stretched elements
Adaptive Time-Stepping and Computational Stability

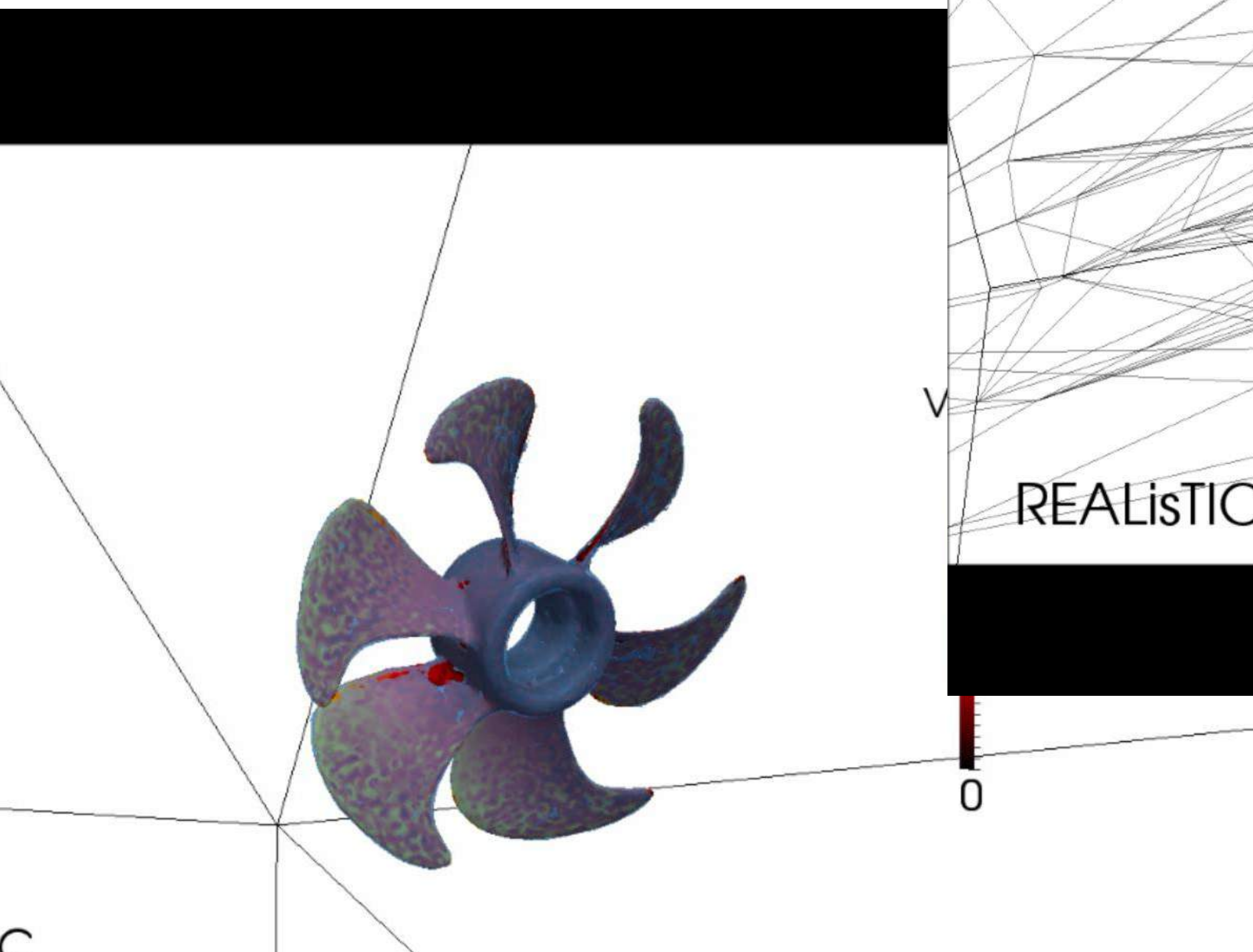

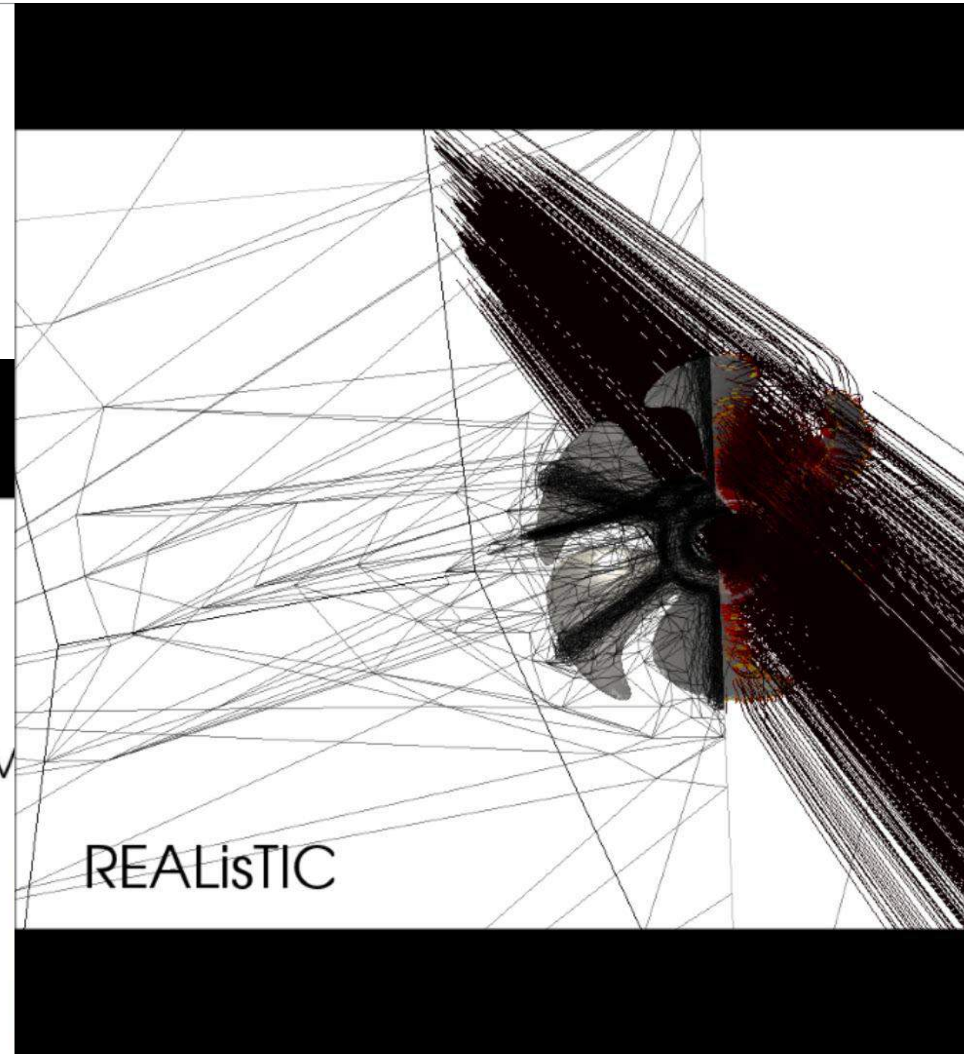

Parallel anisotropic adaptation with moving embedded geometries

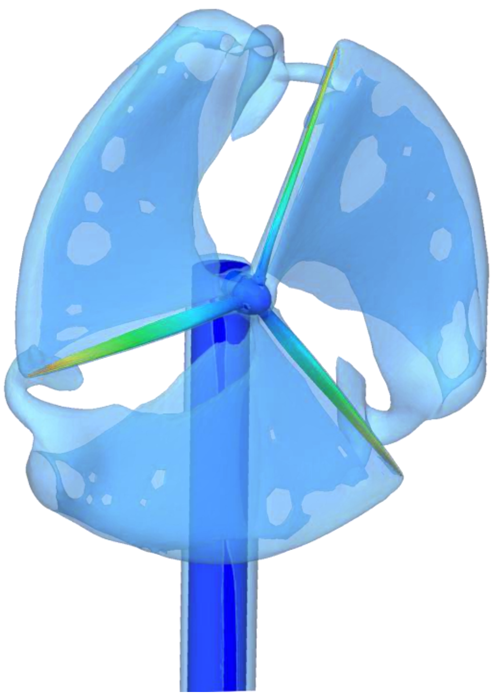

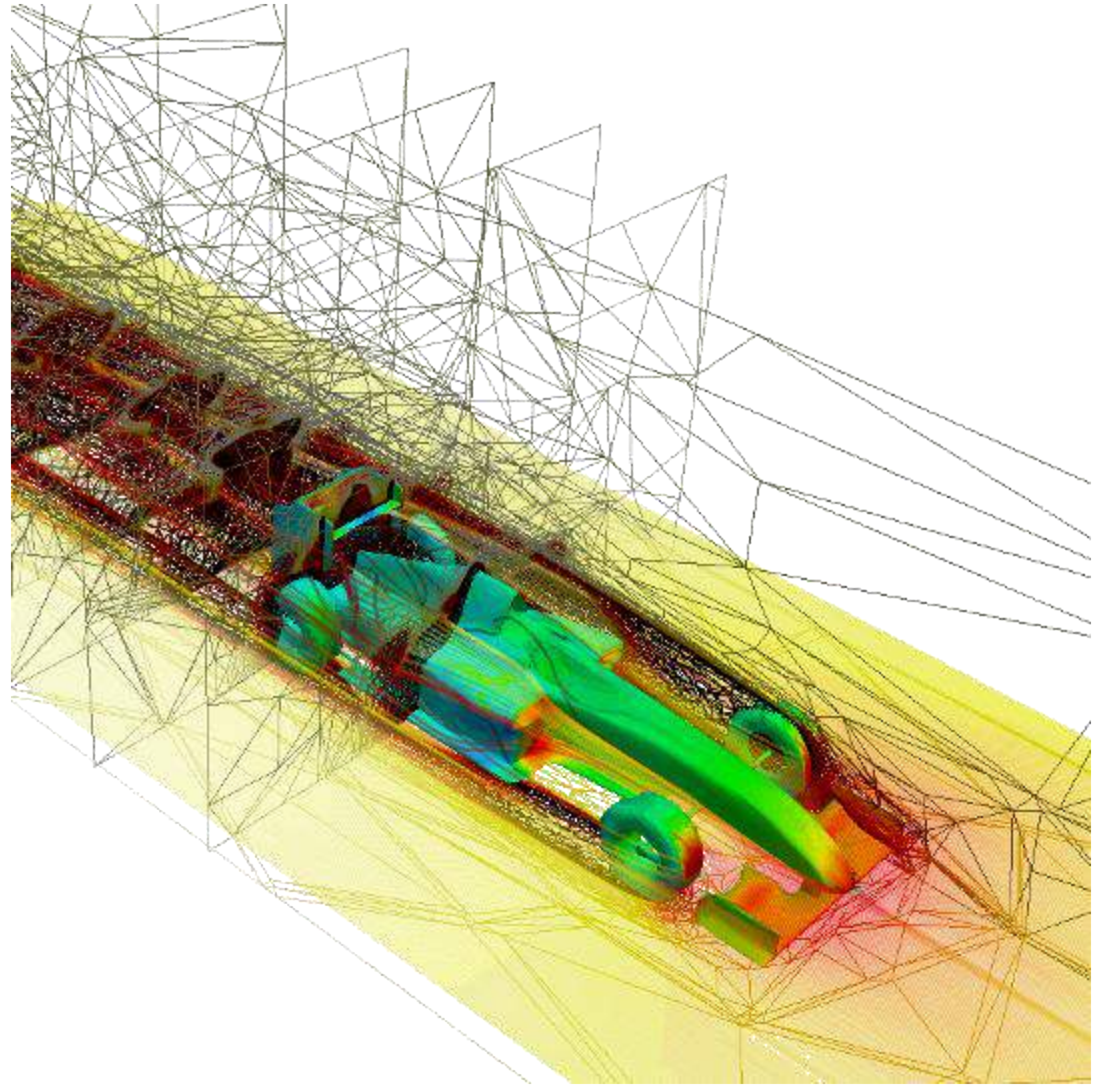

Multiphase flows

- Quenching process
- Turbulent boiling
- Phase change
- vapor film bubbles growth and expansion
- surface tension

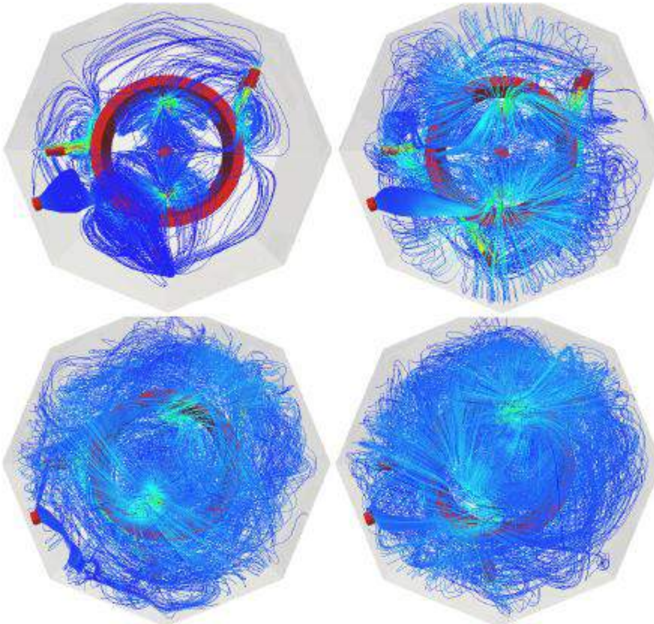

3D quenching of an ingot inside a water tank with agitation (no phase change is considered)

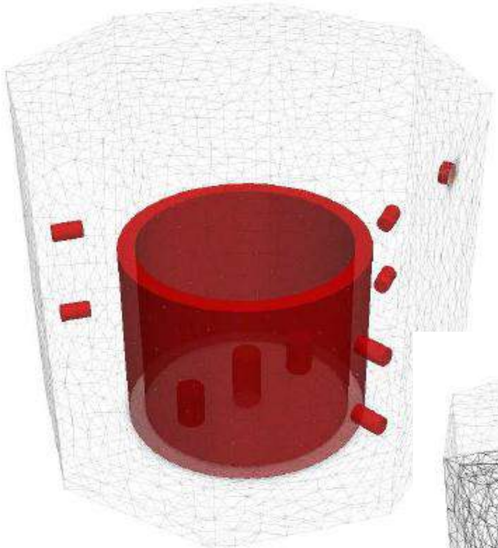

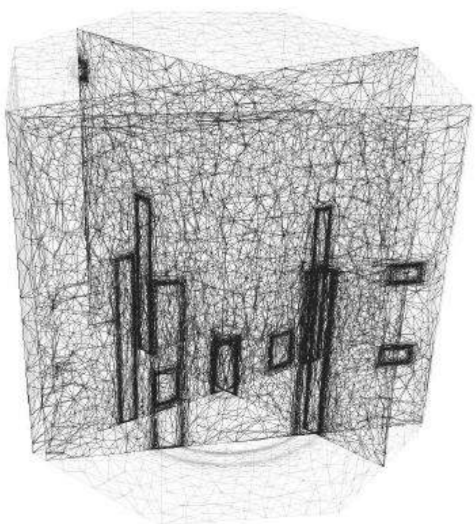

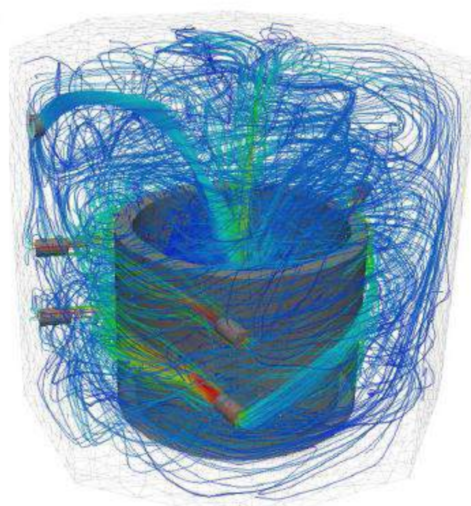

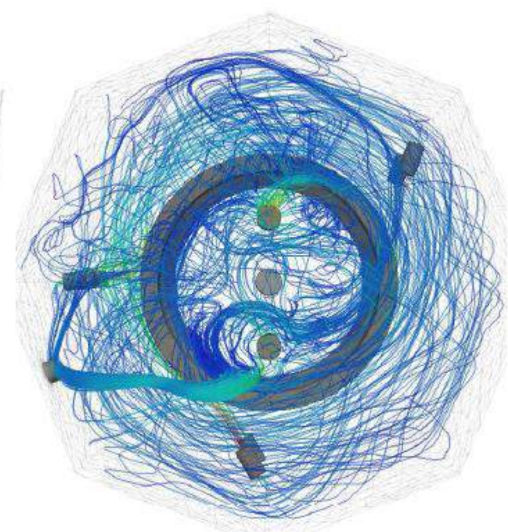

Heat treatment of six ingots inside a furnace (96 cores)

ArcelorMittal
Industeel

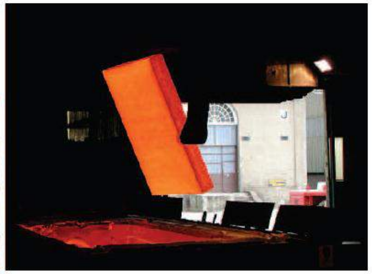

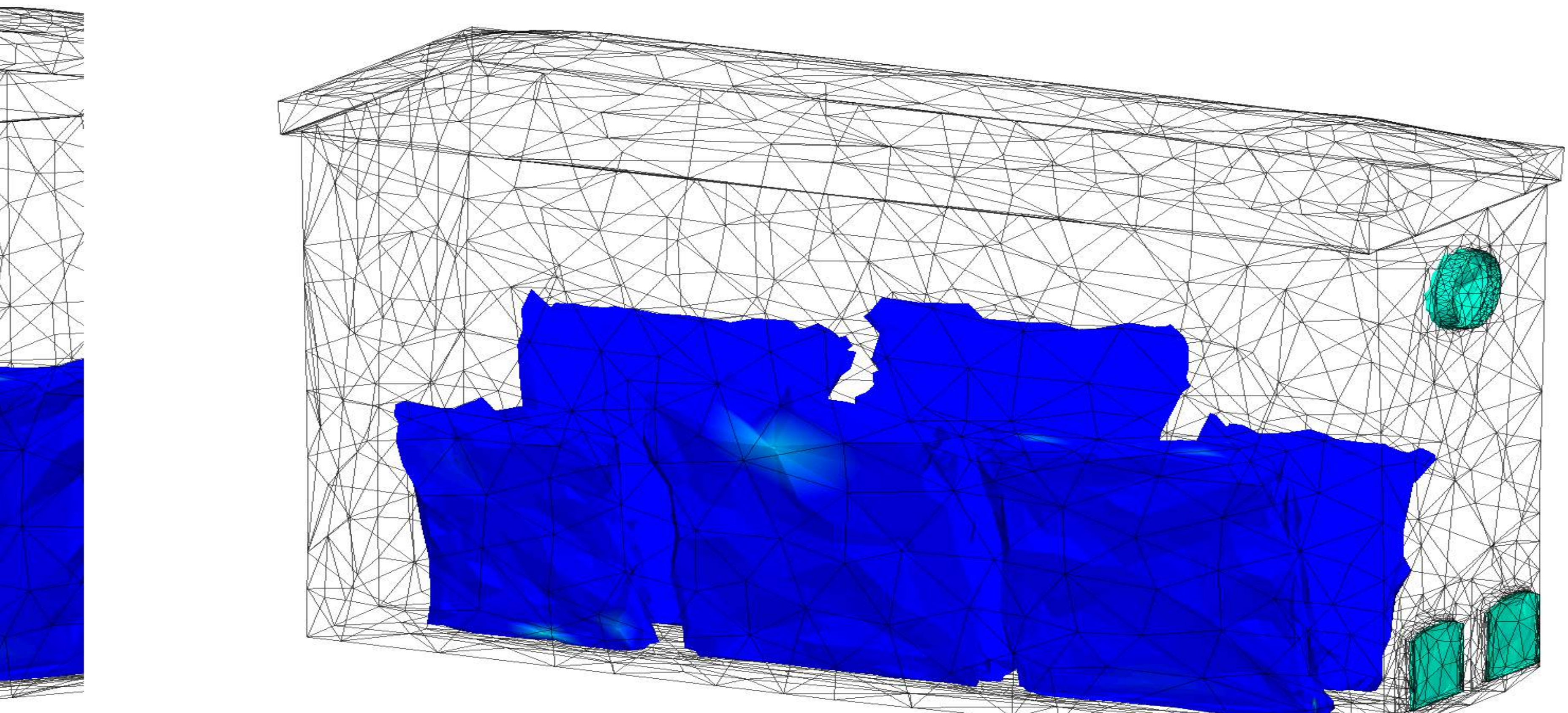

Extreme cases

~22 million nodes

~120 million elements

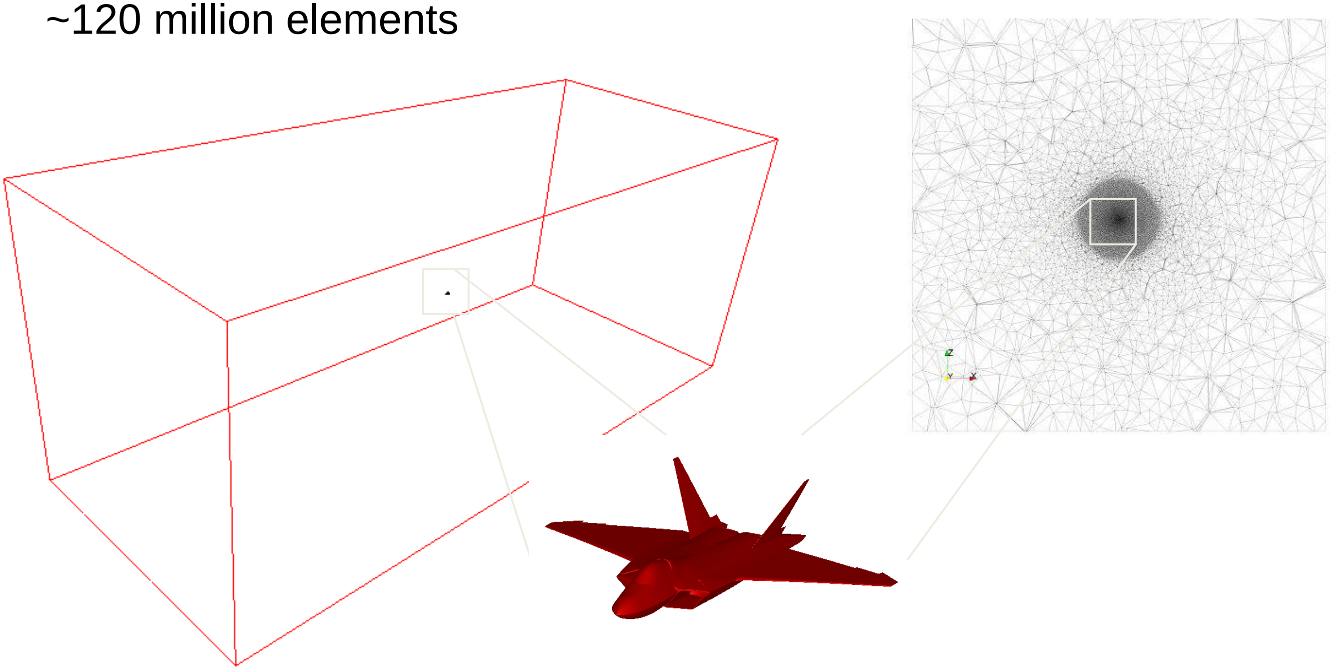

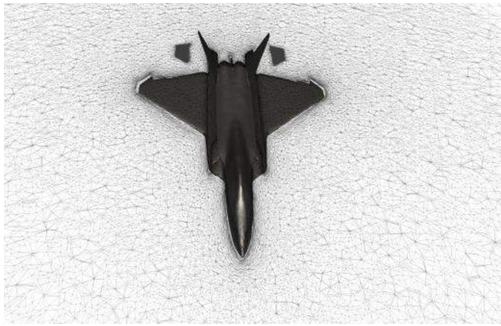

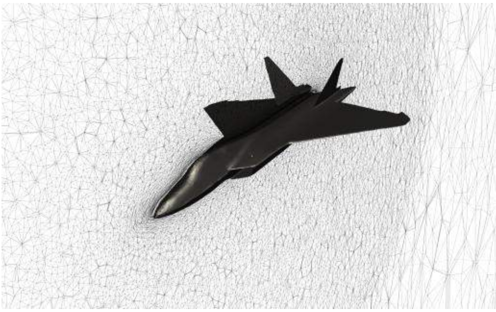

Towards exascale: H2020 FET HPC, GENCI, PRACE

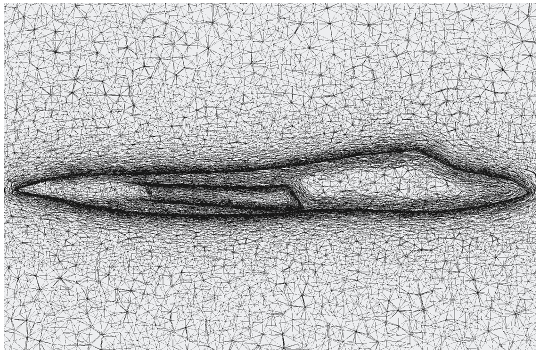

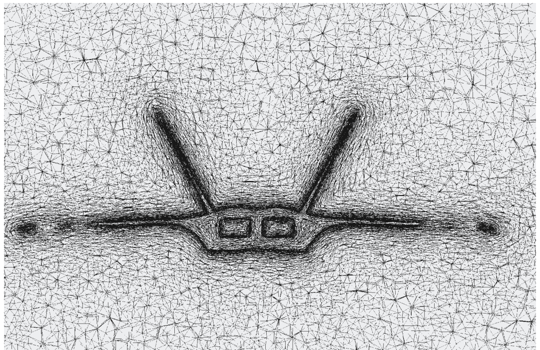

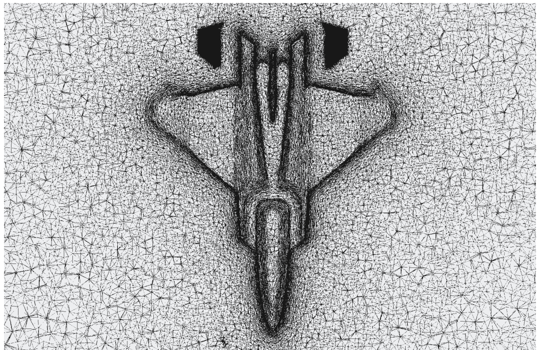

Thank you for your attention (chin chin)

Turbulent multiphase flows

Experiment

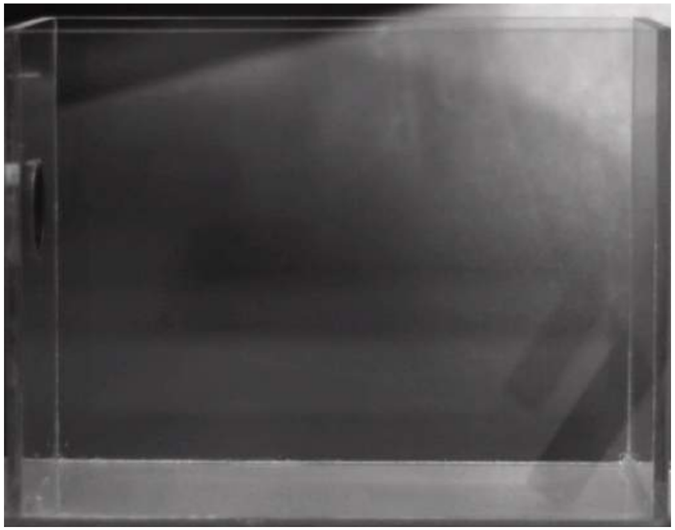

Numerical